

# Micro- and Nanosystems for Advanced Transdermal **Delivery**

Li Yan, Maria Alba,\* Nazia Tabassum, and Nicolas H. Voelcker\*

The skin is the largest and most accessible organ in the human body and, as such, it appears as the most convenient portal for drug delivery. However, the skin is also a formidable barrier which, while protecting us from physical, chemical, and immunological agents, requires appropriate technology for effective delivery. Today, the most effective administration method for large, lipophobic, and polar molecules continues to be hypodermic injection, which is associated with pain, needle phobia, and stick injury. As an alternative, a range of advanced strategies to overcome the skin barrier have been established over the last few decades including chemical enhancement, sonophoresis, iontophoresis, electroporation, thermal ablation, and mechanical approaches. Encouraged by the advances in nanotechnology, micro- and nanosystems have emerged as powerful tools to overcome the skin barrier, enabling significant advances on the existing methods. In particular, microneedle- and nanoparticle-assisted transdermal delivery has gained significant traction and will most likely have a strong impact in the field. In this review, the most recent progress in the field of transdermal delivery based on microneedle and nanoparticle delivery systems is discussed and examples of key therapeutic application are provided. Finally, a critical summary is presented alongside a vision for future research directions.

## 1. Introduction

The great majority of marketed therapeutics consists of smallmolecule (<500 Da) drugs exhibiting high potency and balanced lipophilicity, which favor their bioavailability and site specificity.<sup>[1]</sup> Many other promising drugs, however, have not been translated

Dr. L. Yan, Dr. M. Alba, N. Tabassum, Prof. N. H. Voelcker Monash Institute of Pharmaceutical Sciences

Monash University

Parkville, Victoria 3052, Australia

E-mail: maria.albamartin@monash.edu; nicolas.voelcker@monash.edu Dr. L. Yan, Dr. M. Alba, Prof. N. H. Voelcker

Commonwealth Scientific and Industrial Research Organisation (CSIRO)

Manufacturing

Clayton, Victoria 3168, Australia

N. Tabassum

The University of Central Punjab Johar Town, Lahore 54000, Pakistan

Prof. N. H. Voelcker

Melbourne Centre for Nanofabrication

Victorian Node of the Australian National Fabrication Facility Clayton, Victoria 3168, Australia

The ORCID identification number(s) for the author(s) of this article can be found under https://doi.org/10.1002/adtp.201900141

DOI: 10.1002/adtp.201900141

to the clinic due to their poor therapeutic performance.<sup>[2]</sup> Biological barriers such as the skin, serving as a protective layer to prevent the access of infectious and harmful agents into the human body, are the major obstacles for effective drug delivery to sites of interest.[3] The development of highly efficient delivery routes to overcome biological barriers is becoming an urgent need, and a fundamental transformation on how drugs are administered to patients is expected in the foreseeable future.<sup>[4]</sup> Today, small-molecule drugs are increasingly being replaced by a newest generation of therapeutics notably represented by large biomolecules. Indeed, nearly 30% of the 59 drugs approved by the US Food and Drug Administration (FDA) in 2018 were large molecule biologicals, ranging from oligonucleotides (7 kDa) to monoclonal antibodies (150 kDa).<sup>[5]</sup> Currently, these drugs require invasive methods for their effective administration, and hypodermic injection continues to be the gold standard. The same is true for polar and lipophobic small-molecule drugs.[6] Traditional needle and syringe

injection, however, presents several drawbacks, including the generation of sharp waste, risk of injury and infection, limited efficiency, and causing pain and needle phobia. [2b,6,7] In addition, hypodermic injection usually requires administration by trained healthcare professionals.

Intensive research efforts have focused in finding noninvasive administration methods for large, polar, and lipophobic molecules, such as transdermal, oral, inhalation, and transmucosal approaches. Among these, transdermal administration may be the most attractive and convenient route for drug delivery. The skin is the largest and most accessible organ in the human body and has been used for centuries as a portal for drug delivery, not only for local dermatological conditions, but also for systemic diseases.<sup>[8]</sup> However, the skin is also one a formidable biological barrier and limits the penetration of most therapeutics. The skin contains fine and sophisticated layered structures including the epidermis, dermis, and hypodermis. The stratum corneum, located in the epidermis, is the outmost layer of skin with a thickness of 10–40 μm. This layer is almost impermeable to large (>500 Da), polar, and hydrophilic molecules. [2b,9] The stratum corneum is mostly composed by non-living corneocytes and is constantly renewed. [10] In addition, it is surrounded by multiple lipid bilayers, which creates tortuous hydrophobic sections around the corneocytes.[11] These features critically hinder the

transport of active agents through the stratum corneum. Once this layer is bypassed, the active agents need to cross the viable epidermis and to reach the dermis, where systemic absorption occurs. The viable epidermis mainly consists of cellular components with relatively low cellular interspacing and without vascular and nerve endings. In comparison, the underlying dermis contains blood vessels and nerve terminations, and is responsible for the entire skin metabolism and innervation.<sup>[12]</sup> Consequently, highly efficient transdermal delivery with minimal invasion is a particularly challenging task.

Over the past few decades, a number of advanced techniques have been developed in order to overcome the skin barrier and improve the transdermal drug delivery efficacy. These methods can be categorized as passive, when they rely on diffusion mechanisms to bypass the skin barrier; or active, when they employ a physical disruption to bypass the stratum corneum. Passive methods have traditionally relied on chemical enhancers.<sup>[13]</sup> Transdermal patches are a successful example for the noninvasive, passive delivery of small, potent drugs. However, their efficiency for large molecules is very limited. [6,14] In efforts to translate the success of transdermal patches to larger, polar and/or lipophobic molecules, researchers have recently focused on developing carriers that promote the transport of these bioactives. A range of novel nanoparticle formulations including liposomes,<sup>[15]</sup> polymeric nanoparticles,<sup>[16]</sup> dendrimers,<sup>[17]</sup> micelles,[18] and inorganic nanoparticles have been proposed as passive transdermal drug delivery carriers with encouraging outcomes. Alternatively, a number of active techniques able to disrupt the stratum corneum have been established to facilitate the delivery of molecules impermeable to the skin. Iontophoresis, [19] ultrasound, [20] electroporation, [21] thermal ablation, [22] and jet injection<sup>[23]</sup> have been proven effective to modulate the skin barrier and enable transdermal delivery, but they require complex equipment and specialized personnel, significantly limiting their adoption. Microneedle systems have also demonstrated effective delivery by mechanically disrupting the stratum corneum and assisting active agents to penetrate into the dermis.[24] Those devices present several advantages over other active delivery techniques, as microneedles can be applied by patients themselves, are cost-effective, and require minimal support infrastructure. Indeed, this technology is currently the most widely used for transdermal delivery in laboratory studies and clinical trials.<sup>[25]</sup>

With the rapid development of materials science and nanotechnology, microneedle and nanoparticle systems have gained a prominent position for enhanced transdermal delivery. Here, we will review the developing role of nanotechnology in transdermal drug delivery with a focus on microneedle and nanoparticle systems, as the technologies that most likely will have an impact in the near future. We will provide an update on their recent progress and discuss their versatile therapeutic applications, from local skin conditions to systemic diseases. Finally, we highlight the most significant achievements to date and present our view on future research prospects.

# 2. Microneedle Patches for Transdermal Delivery

Microneedle patches consist of arrays of vertically aligned conical microstructures ranging from tens to hundreds of microns



Maria Alba is a National Health and Medical Research Council (Australia) Early Career Fellow at the Monash Institute of Pharmaceutical Sciences, Monash University, working on the development nano- and microneedle platforms for advanced therapy and diagnosis. Her research has been devoted to the design, fabrication, and application of functional nanomaterials in biosensing and

drug delivery from understanding the principles that govern the interaction with biological systems. She obtained her Ph.D. in 2015 from Universitat Rovira i Virgili, Spain. Before joining Monash University, she worked in Prof. Voelcker's lab at the Mawson Institute of the University of South Australia as a post-doctoral fellow.



Nicolas H. Voelcker is the Scientific Director of the Melbourne Centre for Nanofabrication, Professor at the Monash Institute of Pharmaceutical Sciences, Monash University, and Science Leader at the Commonwealth Scientific and Industrial Research Organisation (CSIRO). His key research interests are the fabrication and surface modification of silicon nanomaterials for applications

in biosensors, biochips, biomaterials, and drug delivery. His research often seeks to address clinical challenges through the application of materials science and nanotechnology.

in length. [6] The length and dimensions of microneedles can be manufactured to perfectly match the structure of skin. Indeed, they have been designed to by-pass the stratum corneum and enable transdermal delivery, while not causing any pain (Figure 1). These microstructures have the ability to physically pierce into the outmost layer of skin, and create microchannels that facilitate the transport and absorption of molecules otherwise impermeable to the skin. [26] With significant improvement over the last 20 years, the microneedle technique is now utilized to transdermally deliver a wide range of molecules including vaccines, anti-cancer drugs, insulin, and cosmetic agents.

Microneedle patches with different shape, composition, geometry, and functionality have been developed. Depending on the design, microneedles can be categorized as: solid, hollow, dissolving, degradable, responsive, and bioresponsive.<sup>[27]</sup> The first report of a microneedle patch for transdermal delivery consisted of solid silicon microneedle arrays and was reported in 1998 by Prausnitz and co-workers.<sup>[28]</sup> In this seminal study, a silicon microneedle patch was fabricated by means of deep

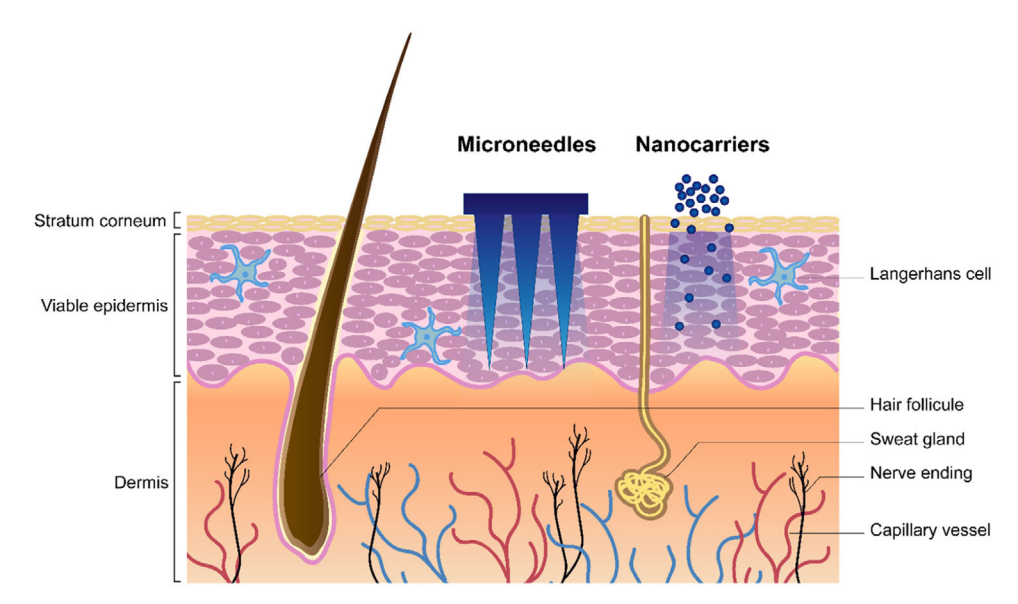
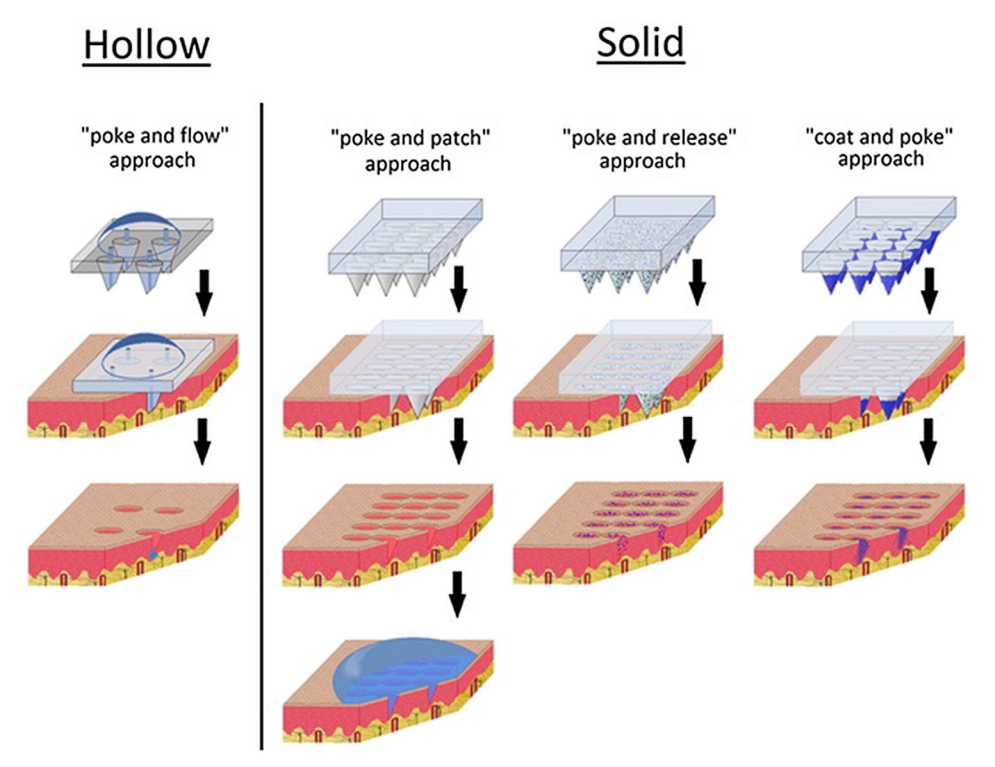


Figure 1. Schematic representation of skin structure together with microneedle and nanocarrier systems for transdermal delivery.

reactive ion etching (DRIE), and demonstrated to enhance the skin permeability of a model drug (calcein) by four orders of magnitude.[28] This work inspired an early generation of transdermal patches that were mainly based on solid microneedles arrays made of silicon or metals. Later, more sophisticated microfabrication methodologies allowed the fabrication of hollow microneedles, which enabled the infusion of liquid formulations and demonstrated increased drug loading capacity.[29] However, silicon and metal microneedles showed limitations, for example high-cost, difficulty of reproducible coating and low loading capacity.[30] Since the early years, polymers have attracted a growing attention for microneedle manufacturing due to their adjustable physico-chemical properties, enhanced biocompatibility, cost-effectiveness, ease of fabrication, and no sharp waste.[31] Similar to their silicon and metal counterparts, polymeric microneedles were first used as to open micro-channels on the skin that increase permeation of active agents after topical application.<sup>[32]</sup> Also, polymeric coatings were introduced in combination with the drug formulation to allow greater control over the loading and release. [33] Later, researchers explored microneedle manufacturing using biodegradable polymers that contain the therapeutic within their matrix and controllably dissolve or degrade upon insertion into the skin. Depending on the polymer dissolution rate, these microneedle arrays can be categorized as dissolving or degradable. Dissolving microneedles are typically made with polymers of high water solubility that dissolve within minutes after contact with the skin, producing a fast release. Dissolving microneedle arrays have been reported using a range of water-soluble polymers including hyaluronic acid (HA),[34] polyvinylpyrrolidone (PVP),[35] polyvinyl alcohol (PVA), carboxymethyl cellulose, [36] chitosan, [37] and maltose. [38] Degradable microneedles are regarded as those with slow dissolution rate, which typically results in extended release profiles. Degradable microneedles have been traditionally achieved by using biocompatible polymers of high molecular weight and/or crosslinking degree such as polylactides. [39] The payload is continuously released via passive diffusion or degradation of the polymeric matrix. Lately, slow release has also been achieved by incorporating materials secondary encapsulation elements (e.g., polymeric nanoparticles, [40] biominerals [41]) within a dissolving matrix. And extensive efforts have been devoted to generate responsive and bioresponsive polymeric microneedles. These responsive microneedle arrays have the ability to release the embedded active agent in response to triggering stimuli. These stimuli may come from an external source or from a physiological event. Externally applied light<sup>[42]</sup> or heat<sup>[43]</sup> signals have been demonstrated to trigger the release of therapeutics loaded within a polymeric matrix. Advanced approaches have also demonstrated that physiological signals, such as variations in pH,<sup>[43]</sup> glucose,<sup>[44]</sup> or reactive oxygen species,<sup>[45]</sup> may be employed to trigger the dissolution of microneedle arrays and release a therapeutic, thus creating bioresponsive systems.

The variety of methods in which these microneedle patches may be applied to the skin for transdermal drug delivery methods have been summarized by Boustra and co-workers, as schematically depicted in Figure 2.[46] In brief, four transdermal delivery approaches can be illustrated known as: 1) "poke and flow," when the drug containing solution is actively or passively delivered through the bore of the hollow microneedle; 2) "poke and patch," when the drug passively diffuses via the micropores created by the penetration of microneedles into skin tissue; 3) "poke and release," when the dissolving or biodegradable microneedle penetrate into skin and subsequently release the drug following microneedle dissolution; and 4) "coat and poke," when the drug is coated onto a non-dissolving microneedle surface and drug released from microneedle surface after microneedle penetration into skin.[46] Currently, "poke and release" and "coat and poke" are the two most prominent approaches for microneedle patch application. This is possibly because they are more cost-effective and have superior transdermal delivery efficacy.

In the next sections, a detailed description of the latest advances on microneedle array technology for disease treatment is provided.



**Figure 2.** General approaches for transdermal delivery by hollow and solid microneedles. Illustrated on the left is the "poke and flow" approach, where a drug containing solution is actively or passively delivered through the bore of hollow microneedles. Solid microneedles may be used in three different manners: "poke and patch" approach, where micropores are first generated in the skin by microneedle patch application, then the drug is topically applied to passively diffuse through these micropores; "poke and release" approach, where dissolving or biodegradable microneedles release the drug by dissolution of the microneedles in the skin; and "coat and poke" approach, where drug-coated microneedles are pierced through the skin, and then the drug is released into the skin through hydration of the coating. Reproduced with permission. [46] Copyright 2012, Elsevier.

## 2.1. Microneedle Patches for Transdermal Vaccine Delivery

A vast number of hazardous pathogens including viruses and bacteria surround humans day in day out, which collectively results in high probability of infection. Vaccination, a process of exogenously stimulating immune responses, has dramatically improved the management of infectious diseases. Although traditional intramuscular needle and syringe injection is still the most common and convenient administration route for skin delivery, this approach has some considerable disadvantages and risks, as mentioned above. To address those problems, microneedle patches emerged as a powerful technique for transdermal vaccine delivery, due to their simple and minimally invasive administration, together with low cost and reduced risk of infection.

There are additional merits of using microneedle patches for vaccine delivery. For example, microneedle patches can directly deliver vaccine into the upper layer of skin, a tissue region with abundant antigen presenting cells, thus significantly increase the immune response. <sup>[12,50]</sup> The first study of in vivo use of a microneedle patch to penetrate skin and deliver vaccine was conducted by Mikszta et al. in 2002. <sup>[51]</sup> In this work, silicon-based microneedle arrays were applied to breach the skin with minimal discomfort and irritation. As tested in a mouse model, microneedles effectively delivered plasmid DNA with 2800-fold above topical controls. In addition, the authors also demonstrated that with the help of microneedle patches, topical immunization with

naked plasmid DNA could induce stronger and reliable immune responses. Distinct from traditional needle and syringe administration that stores vaccine in liquid form, the vaccine is stored in a dried form on/in the microneedle, and dissolves in the dermis after application into skin. Vaccine stored in dried form is more stable than liquid form, and is potentially suitable for coldchain free storage. [52] For example, Chen et al. dry-coated influenza vaccine on microneedles with 32.5% transdermal delivery efficiency.<sup>[52a]</sup> Compared with intramuscular injection with needle and syringe, microneedle technique could achieve equivalent protective immune response with 1/30th of a dose. Also, influenza vaccine that coated on microneedles for 6 months at 23 °C induced comparable immunogenicity with freshly coated microneedles, corroborating the long-term thermostabilization. [52a] Recently, Poirier et al. fabricated a dissolving microneedle patch made of hydroxyethyl starch and chondroitin sulphate, and incorporated hepatitis B surface antigen formulated with saponin QS 21 as adjuvant. [53] The thermostability of this microneedle patch was evaluated for storage at 37, 45, and 50 °C for up to 6 months. Antigenicity was well retained at 37 and 45 °C and only 10% loss was observed at 50 °C.[53] Cold-chain free vaccine storage of microneedle patch is desirable because it reduces the cost of vaccination, and makes vaccine accessible also to developing countries, where a cold-chain supply is often lacking.

To date, the two most used microneedle types for vaccination are i) solid non-degradable and removable microneedle patches; and ii) dissolving/degradable microneedle patches. Solid

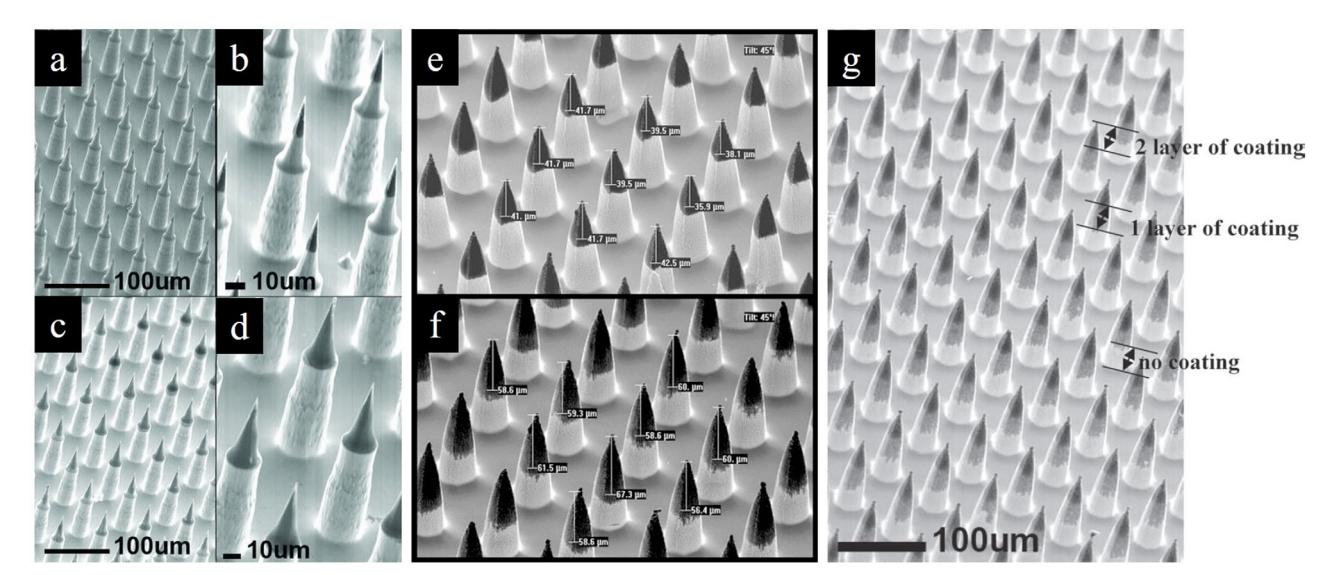


Figure 3. Scanning electron microscopy images of site-selectively coated microneedles. a–d) Microneedles coated with DNA; e,f) microneedles coated with OVA protein; g) microneedles coated with two layers of dextran: a first layer was coated on the top 40  $\mu$ m of the microneedles; a second layer of dextran was coated on the top 70  $\mu$ m of the microneedles. This demonstrates that the thickness and length of the coating can be controlled by the deposition technique. Reproduced with permission. Copyright 2011, Wiley-VCH.

non-degradable and removable microneedle patches are usually made of metals or silicon. [46,54] Vaccine formulations are coated onto the solid non-degradable microneedle surface.<sup>[55]</sup> The coating technique is crucial: vaccine coated on the bottom and substrate of patch cannot be delivered to the skin, and only the formulation remaining on the top of microneedles may penetrate the skin and evoke an immunological effect. Vaccine formulations are expensive and sometimes in limited supply. Thus, selective coating of the microneedle tip is a cost-effective and dose-sparing approach, but it is technologically challenging. To solve the problem, several dry-coating methods have been developed to selectively coat the tip of microneedles with different biomolecules and vaccine. [56] For example, Chen et al. reported a simple dip-coating technique able to tune the coating length on the microneedle tip by controlling coating solution viscosity (Figure 3).<sup>[55a]</sup> By using this coating technique, molecules representative of vaccines (e.g., chicken egg ovalbumin (OVA) protein, DNA, and fluorescent dyes) were successfully coated onto the microneedle tip in a controlled way. After skin application, 82.6% in mass of vaccine coated was rapidly released from the microneedles to the skin within 2 min, and an immune response was generated upon delivery of influenza vaccine (Fluvax) in a mouse model.[55a] As an alternative to solid non-degradable and removable microneedle patches, vaccine formulations may be incorporated into the matrix of dissolving/degradable microneedle patches. Prausnitz and co-workers reported the first successful fabrication of fast dissolving microneedles made of PVP and carboxymethyl cellulose for vaccine delivery.[35,57] For dissolving microneedle patches made of various materials (carboxymethyl cellulose,<sup>[58]</sup> PVP,<sup>[35,59]</sup> silk,<sup>[60]</sup> HA,<sup>[34]</sup> etc.) vaccine formulation is typically encapsulated in a polymer casting approach.

In recent years, the fit-for-purpose performance of both solid non-degradable and removable microneedle arrays and dissolving/degradable microneedle for vaccine delivery has been demonstrated extensively in both in vitro and in vivo studies. For example, vaccine-delivering microneedles have been tested in the context of infectious diseases, including human papilloma virus (HPV),[61] DNA-delivered attenuated west Nile virus, [62] inactivated rotavirus, [63] hepatitis B/C, [53,64] Bacillus Calmette-Guérin, [65] influenza, [66] measles, [67] poliovirus, [52b,68] and Ebola.[40] Recently, a microneedle patch was designed to co-deliver vaccine and a cytokine adjuvant (granulocytemacrophage colony stimulating factor (GM-CSF)) for improved vaccination. [66b] In this study, dissolving microneedles were mixed with GM-CSF-adjuvanted influenza vaccine for skin immunization. It was found that those microneedles induced robust and long-lived antibody responses. [66b] In another study, an Ebola DNA vaccine formulation was coated onto polylactic-co-glycolic acid—poly-1-lysine/poly-γ-glutamic acid (PLGA-PLL/γPGA) nanoparticles and incorporated into PVA microneedle patch.[40] A stronger immune response and increased stability compared with conventional intra-muscular administration of Ebola DNA was reported. Chen et al. designed antigen-loaded chitosan microneedle tips on top of hydrophilic PVA/PVP supporting microneedle array patch (Figure 4).[69] The microneedles remained in the dermal layer and allowed sustained release for up to 28 days. [69] In addition, the efficacy of the microneedle vaccine delivery technique was evaluated in non-human primates (macaques) in 2013.[70] Here, a microneedle patch made of bioresorbable poly(L-lactic acid) (PLA), and surface-coated with adenovirus type 5 (Ad5) vector vaccine produced a strong cellular and humoral immunity in macaques, equivalent to traditional intramuscular injection.<sup>[70]</sup>

## 2.2. Microneedle Patches for Diabetes Therapy

Diabetes mellitus is a metabolic disorder characterized by the low clearance of glucose in muscle and fat tissues caused by the abnormal secretion of insulin. Today, diabetes affects one

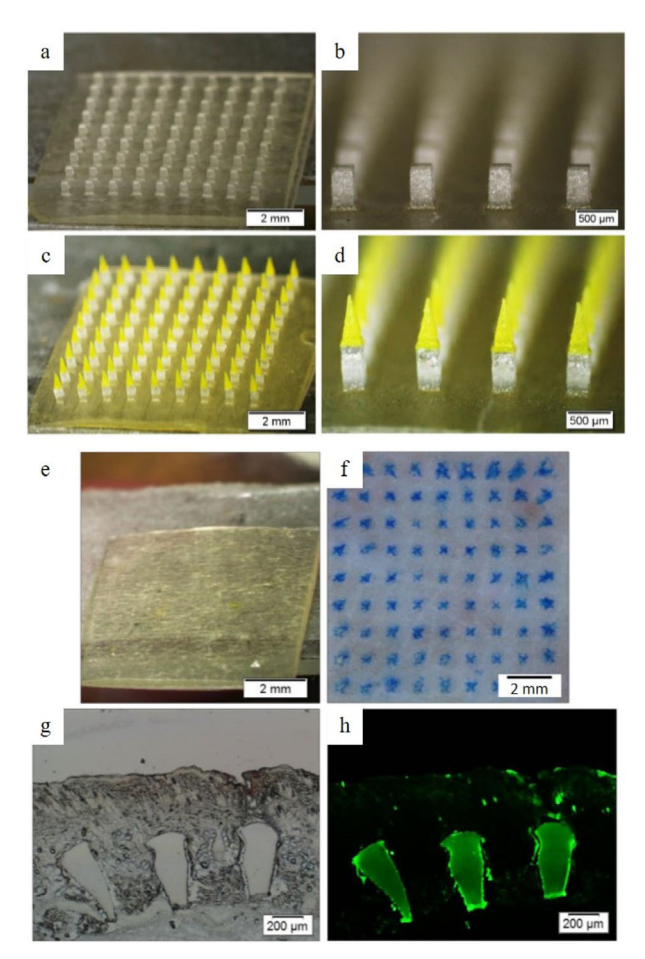


**Figure 4.** Dissolving antigen-loaded chitosan microneedles. a,b) Brightfield micrographs of the PVA/PVP supporting array patch; and c,d) Fluorescein isothiocyanate (FITC)-labeled chitosan microneedles integrated with the hydrophilic PVA/PVP supporting array. e–h) Skin penetrations tests. Bright-field micrographs of the microneedle array after application to a porcine cadaver skin for 5 min (e); and the treated skin after microneedle patch application and blue tissue marking staining (f). Histological sections of the rat skin after application of the FITC-labeled chitosan microneedles (g, h): bright-field (g) and fluorescence (h) micrographs, displaying green fluorescence corresponding to FITC emission. Reproduced with permission. [69] Copyright 2018, Elsevier.

in eleven adults and this ratio is expected to continue to grow over the next decades.<sup>[71]</sup> The disease is generally caused by the deficient function of the pancreas and characterized by insufficient insulin secretion (type 1) or by the ineffectiveness of insulin (type 2).<sup>[72]</sup> Exogenous administration of insulin is currently essential for managing both types of diabetes. Typically, insulin is self-administered by patients via subcutaneous injection several times a day. This is not only associated with pain, risk of infections and injuries but also requires training and rigorous self-management. In their search for novel, patient-friendly routes, researchers have proposed microneedle patches as a minimally-invasive and convenient method to deliver insulin into the bloodstream.<sup>[73]</sup>

Early generations of transdermal patches for the delivery of insulin consisted of solid microneedles. For example, Prausnitz and co-workers applied a solid metal microneedle patch in a

"poke and patch" approach for the delivery of insulin to live diabetic rats.<sup>[74]</sup> Microneedles demonstrated an increased efficiency lowering the blood glucose levels compared to passive delivery across untreated skin. Later, hollow microneedles were also applied for the delivery of insulin. Metallic hollow microneedles were fabricated in a multi-step process involving polymer molding, metal deposition, and polymer etching. Using such a microneedle architecture to deliver insulin achieved reductions in blood glucose levels to almost 50% of the initial value over a 4 h period.<sup>[75]</sup> More recently, Resnik et al. established a methodical protocol for the administration of insulin using a hollow microneedle patch to human subjects. In healthy individuals, insulin delivery using these hollow microneedle patches was more efficient and led to smoother blood glucose profiles compared to subcutaneous delivery.<sup>[76]</sup> Clinical trials in patients with type 2 diabetes have also been conducted to further assess the safety and efficiency of hollow microneedles.<sup>[77]</sup> Apart from showing a good safety profile, hollow microneedle-based injection showed superior pharmacokinetics compared to conventional subcutaneous administration.

Microneedle arrays have also been fabricated with highly-soluble polymers (HA,<sup>[78]</sup> PVP,<sup>[79]</sup> PVA,<sup>[39a]</sup> gelatin<sup>[80]</sup>) that contain insulin within their matrix. These polymers have also been combined with dissolving glycopolymers for the delivery of insulin (e.g., starch/gelatin,<sup>[81]</sup> maltose/alginate<sup>[39b]</sup>). Ling and Chen established a dissolving microneedle patch made of starch and gelatin.<sup>[81]</sup> They proved that the polymer formulation exhibited sufficient mechanical strength to penetrate in vivo porcine skin, while dissolving within 5 min. Insulin activity was preserved in the fabrication process and the formulation was stable for over a month

One of the recurrent issues in transdermal drug delivery via microneedle patches is the inefficient delivery caused by the incomplete microneedle array insertion into the skin due to the inherent skin elasticity. Kusuma and co-workers established an insertable microneedle patch comprised of arrays of PVA/PVP cylindrical supporting structures capped with conical tips made of insulin-loaded poly-γ-glutamic acid.<sup>[82]</sup> The supporting arrays provide extended length to minimize the skin compressive deformation during application, allowing the tips to reach the dermis. The microstructures dissolved within 4 min when inserted into the skin, releasing their insulin content. The in vivo performance of the system was tested in diabetic rats by applying the patches once a day for 2 consecutive days. The observed hypoglycemic effect was comparable to that of subcutaneous insulin injection in a rat control group, confirming the feasibility and accuracy of the proposed delivery system. Recently, Guo and co-workers reported a microneedle system where microneedle tips readily separate from supporting structures for the controlled release of insulin.<sup>[80]</sup> Microneedle arrays made of genipin-crosslinked gelatin were mounted on supporting PVA-coated polylactic acid microneedle arrays. The use of genipin as a crosslinker enhanced the hydrophobicity and mechanical stability of the microneedles without compromising their biocompatibility. Upon insertion, the PVA coating dissolved within 2 min and allowed the release of the insulin-loaded gelatin microneedle tips from the polylactic acid supporting array, which remained inserted into the skin. The release rate was controlled by tuning the degree of crosslinking: higher degree of crosslinking led to slower

www.advancedsciencenews.com

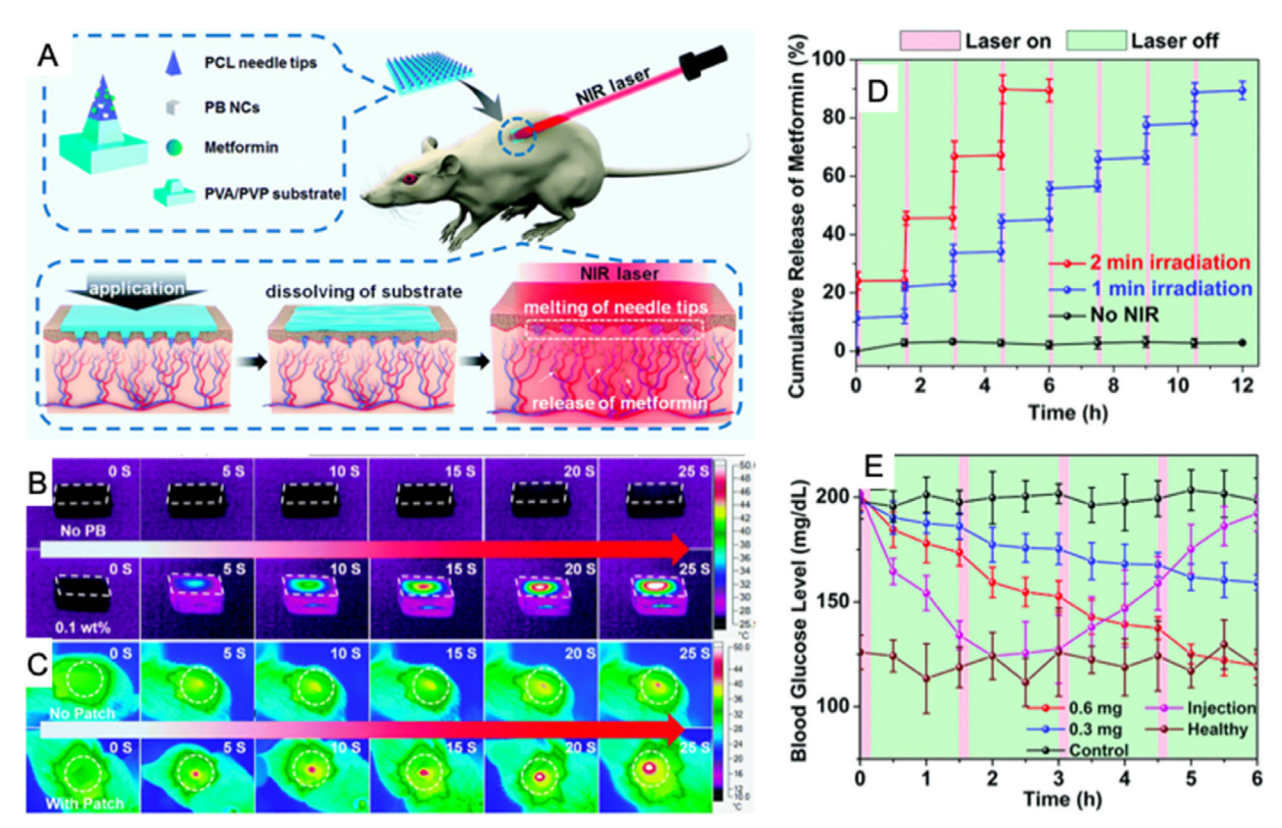


Figure 5. NIR-triggered microneedle system for the delivery of metformin to diabetic rats. A) Schematic illustration of the design and working principle of the NIR-responsive and separable microneedle array system. Following application, the tips remain into the skin and the heat generated by NIR irradiation causes the melting of the needle tips and the release of metformin. B,C) Thermal imaging of mice with (B) and without (C) NIR-responsive microneedle patches under a 0.4 W cm<sup>-2</sup> NIR irradiation in the first 25 s. D,E) NIR-triggered release of the hypoglycemic drug from the microneedle system. Cumulative release of metformin after 1 or 2 min NIR irradiation in vitro (D). Blood glucose levels in diabetic rats after application of 0, 0.3, 0.6 mg of metformin-loaded microneedles and NIR irradiation over four cycles, and their comparison with blood glucose levels in a rat injected with 0.6 mg of metformin and in a healthy rat. Reproduced with permission. [42] Copyright 2017, The Royal Society of Chemistry.

release rate and a prolonged hypoglycemic effect in diabetic mice.

Extended insulin release profiles have been achieved by using degradable microneedle arrays[32,83] Recently, Lu and coworkers have proposed the use of fibroin to fabricate silk fibroin microneedles.<sup>[84]</sup> Proline was used together with fibroin in order to modify the silk crystal structure and therefore control their degradability. Indeed, crystallinity correlated with the insulin release rate, and maintained released were achieved for up to 60 h. The incorporation of bioceramics in dissolving polymeric matrices for controlling the release rate of insulin has attracted attention due to their suitable biocompatibility and excellent mechanical properties.<sup>[41,85]</sup> Liu et al. introduced calcium carbonate microparticles in a PVP matrix to create bioceramic composite microneedles.<sup>[85a]</sup> The hybrid organic-inorganic patches demonstrated slow dissolution for an extended delivery of insulin, with a maximum blood insulin concentration reached after 3 h of microneedle administration, compared to 1 h after subcutaneous injection. Parallel results have been observed for hydroxyapatite/gelatin<sup>[85b]</sup> and calcium sulfate/gelatin<sup>[85c]</sup> hybrid microneedle patches.

Near-infrared (NIR) light responsive composite microneedles have also been proposed to enable on-demand transdermal delivery for diabetic patients. [42,86] NIR irradiation provides good tissue

penetration while causing negligible damage. These microneedle systems typically consist of a photothermal agent and a drug embedded into a dissolving polymer matrix. The photothermal agent (e.g., organic molecules, quantum dots, etc.) has the ability to absorb NIR light and convert it into heat. This heat typically induces the dissolution of the needles and subsequent drug release. Yu et al. proposed a NIR-triggerable and separable microneedle system for the transdermal delivery of metformin, a hypoglycemic drug (Figure 5).[42] The arrowheads of the microneedle arrays were fabricated with a composite consisting of PVA/PVP polymer loaded with NIR-responsive Prussian blue nanoparticles and metformin. Following skin application of the patch, the separable arrowheads remained inserted in the viable layers of the skin. Upon NIR light irradiation, the PVA/PVP polymer dissolved and caused the on-demand release of metformin. This is a promising strategy for the triggerable release of antidiabetic drugs but the fact that high local temperatures (up to 65 °C) are reached may limit the delivery of certain molecules such as peptides and proteins. For instance, this strategy is not suitable for the delivery of insulin as high temperatures may cause its inactivation.

Beyond the light-triggered delivery of hypoglycemic drugs, in recent times there has been an increasing effort in developing microneedle-based glucose-responsive insulin delivery systems.<sup>[44,87]</sup> These bioresponsive microneedles will potentially

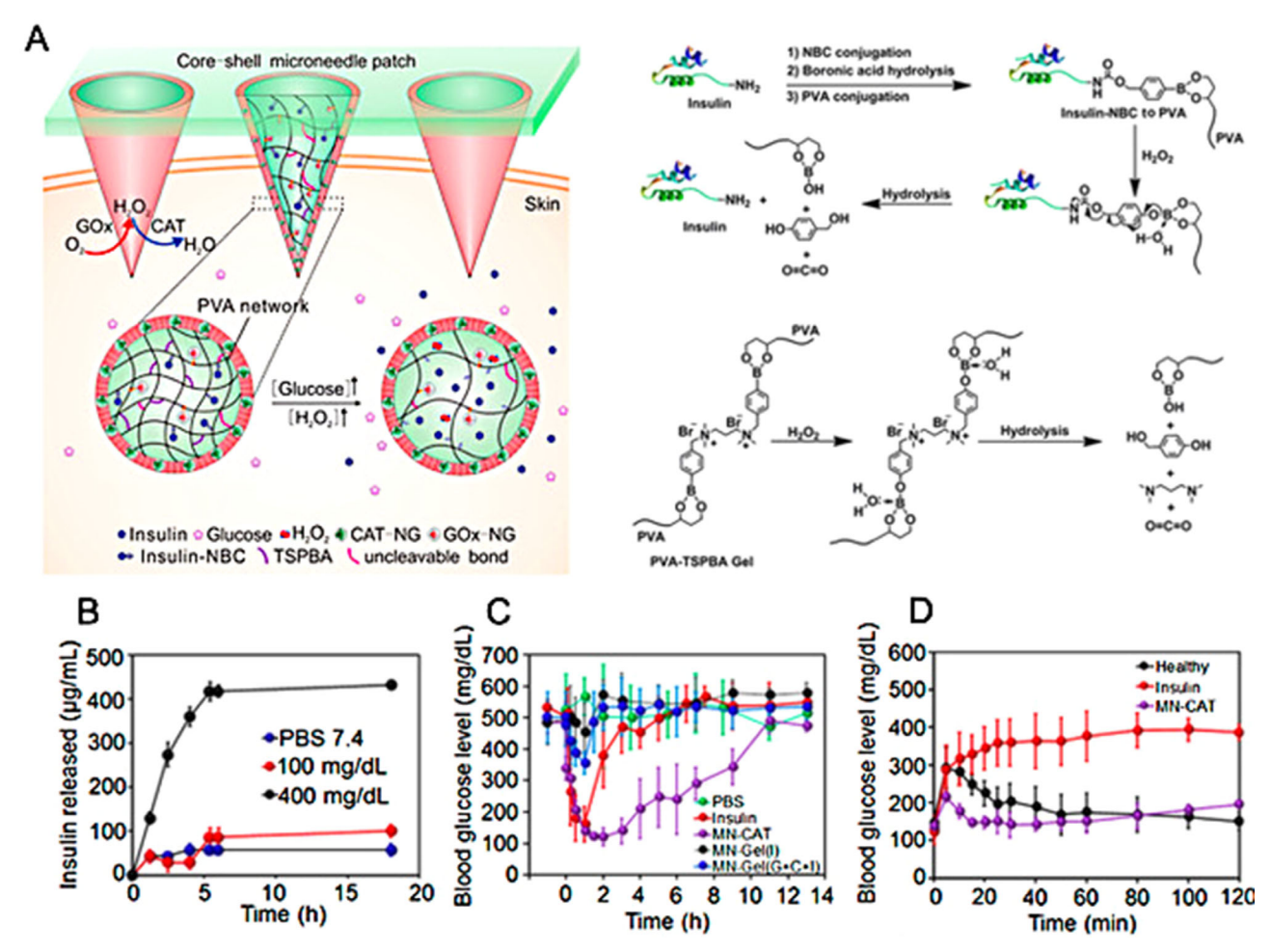


**Figure 6.** Glucose-responsive microneedle insulin delivery system design and in vivo evaluation. A) Schematic representation of the microneedle patch design and working principle. The enzymatic reaction between glucose and  $GO_x$  generates  $H_2O_2$  as a byproduct, which activates the dissolution of the PVA-TSPBA gel matrix. Insulin-NBC anchored to the PVA is also hydrolyzed upon exposure to  $H_2O_2$ , thus releasing free insulin at high glucose levels. The presence of catalase facilitates the elimination of  $H_2O_2$  thus reducing local inflammation. B) In vitro release profile of insulin from PVA-TSPBA gels in PBS pH 7.4 in the presence of  $GO_x$  (0.2 mg mL<sup>-1</sup>) at different glucose concentrations (0, 100, and 400 mg dL<sup>-1</sup>). C,D) In vivo tests of microneedle array patches for type 1 diabetes treatment. Blood glucose levels of diabetic mice (C) treated with PBS, subcutaneous injection insulin, and different kinds of microneedle patches: microneedle arrays formed by a catalase-embedded PVA-TSPBA shell and a core containing  $GO_x$ -nanogel and insulin-NBC (MN-CAT); microneedle arrays of insulin-NBC-loaded gels (MN-Gel(I)); and microneedle arrays of  $GO_x$ -nanogel, insulin-NBC, and CAT-nanogel-loaded gels without a shell (MN-Gel(G+C+I)), n = 5. Glucose tolerance test at 1 h after insulin treatment via either a microneedle patch (MN-CAT) or subcutaneous injection (D). Healthy mice were employed as a control. Reproduced with permission. [87f] Copyright 2018, American Chemical Society.

mimic the physiological response to changes in blood glucose levels and release insulin on-demand. In a typical system, insulin-loaded polymeric microneedles incorporate glucose-responsive triggers. Upon fluctuations in glucose levels, the system responds by releasing the insulin cargo through microneedle dissolution or swelling. The first reported successful approach in combining a microneedle patch with glucose-responsive materials was by Yu et al. [44] Vesicles integrating insulin and glucose oxidase ( $\mathrm{GO}_x$ ) were loaded into hypoxiasensitive HA microneedles conjugated with 2-nitroimidazole. Under a hypoxic environment, hydrophobic 2-nitroimidazole is converted into hydrophilic 2-aminoimidazole. In the presence of high glucose levels, the local hypoxic microenvironment caused by the oxygen consumption in the catalytic reaction of glucose to gluconic acid promoted the bioreduction of 2-nitroimidazole

and the dissociation of the HA-derivate vesicles, with the subsequent release of insulin. The drop in the microenvironment pH caused by the reaction of glucose to gluconic acid has also been exploited to trigger the release of insulin. [87b] Likewise,  $\rm H_2O_2$ , a byproduct of the catalytic reaction, may be employed to trigger the release of insulin.  $\rm H_2O_2$ -responsive polymeric matrixes integrating insulin and  $\rm GO_x$  have been used in glucose-sensitive systems. The released  $\rm H_2O_2$  caused the polymer degradation under increased glucose levels. [87c-e] However, the production of  $\rm H_2O_2$  may irreversibly reduce  $\rm GO_x$  activity leading to a poorly reproducible response to hyperglycemic conditions. In an attempt to regulate this effect, Gu and co-workers integrated a second enzyme, catalase, which acts as a  $\rm H_2O_2$ -scavenging enzyme. [87f,88] In their core–shell approach, microneedles consisted of a  $\rm H_2O_2$ -responsive core matrix loaded with  $\rm GO_x$  and insulin

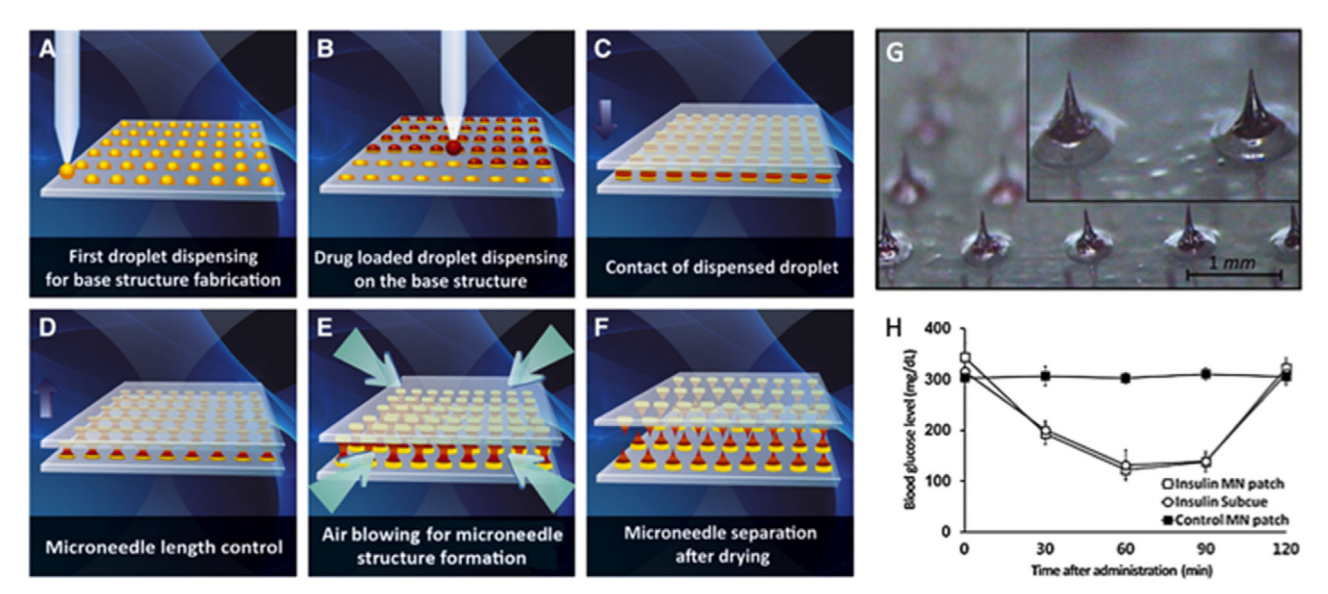


**Figure 7.** Transdermal microneedle based on droplet-born air blowing technique. A–F) Schematic illustration of the microneedle patch fabrication, starting from the deposition of biopolymers arrays (A) followed by co-localized dispensing of the drug-loaded polymer (B). A parallel upper plate makes contact with the polymer arrays (C) to then move upward to create microneedles of controlled length (D). The microneedles are solidified into a conical shape by air blowing (E) and finally the upper and lower plates are separated (F). G) Optical micrograph of the resulting dissolving microneedles arrays. H) Blood glucose levels of mice after the application of bare dissolving microneedles (filled square), insulin-loaded microneedles (2.0 IU kg<sup>-1</sup>, open square) and subcutaneous injection (2.0 IU kg<sup>-1</sup>, open circle). Reproduced with permission.<sup>[89]</sup> Copyright 2013, Elsevier.

whereas the shell was comprised of a catalase nanogel designed to scavenge the excess of H2O2 (Figure 6). H2O2-responsive insulin release was achieved via the modification of insulin with 4-nitrophenyl 4-(4,4,5,5-tetramethyl-1,3,2-dioxaborolan-2yl) benzyl carbonate (insulin-NBC) and subsequent anchoring to PVA. When increased local levels of H2O2 are generated by GO<sub>x</sub> at high glucose concentration, the insulin-NBC-PVA matrix hydrolyzes and free insulin is rapidly released. PVA was also gelated with N1-(4-boronobenzyl)-N3-(4-boronophenyl)-N<sup>1</sup>,N<sup>3</sup>,N<sup>3</sup>-tetramethylpropane-1,3-diaminium another H<sub>2</sub>O<sub>2</sub>-responsive polymer, to maintain the mechanical integrity of the shell structure (Figure 6A). In vivo, this microneedle patch demonstrated euglycemic levels for almost 6 h while minimizing inflammation caused by the H<sub>2</sub>O<sub>2</sub> generation.<sup>[87f]</sup> Apart from the toxicity associated to H<sub>2</sub>O<sub>2</sub>, enzymatic glucoseresponsive systems based on GO<sub>x</sub> present other limitations such as limited long-term stability and poor control over the release rate. Recently, Matsumoto and co-workers have proposed a non-enzymatic microneedle system made from phenylboronic acid-based hydrogels that enabled both sustained and acute glucose-responsive insulin delivery.[87g] They demonstrated 2-month stability in aqueous environments (PBS, pH 7.4, 37 °C). and insulin release highly synchronized with the glucose profile.

As an alternative to the traditional casting method using a micromolding approach, [32] an innovative fabrication approach, so-called droplet-born air blowing, was proposed by Kim and co-workers to directly shape the drug-containing polymers into microneedle tips via air blowing (**Figure 7**). [89] The method allowed rapid (<10 min) microneedle arrays fabrication under mild conditions (4-25 °C), which favors the preservation of the activity of the active agent. The biopolymer, composed of carboxymethylcellulose, HA, and PVP, was dispensed in droplets

in an ordered array as a base layer. A second layer of the same biopolymer droplets containing insulin was then deposited on top. The droplets were drawn to shape into microneedle arrays between two parallel plates by air blowing. The amount of insulin was finely controlled by adjusting the pressure and time of droplet dispenser and the air blowing. In a mouse model, the observed bioavailability of insulin and downregulation of glucose using a microneedle patch fabricated by the droplet-born air blowing method was comparable to that produced by subcutaneous injection. Another novel manufacturing approach was introduced by Yang et al. to create dissolving microneedles from micropillar arrays via the air blowing method.[90] First, a layer of PLGA was electrospun on the pillars; then, droplets of dissolving HA were deposited on each pillar and subsequently shaped into sharpened tips via a droplet-born air blowing process. Aided by the fibrous PLGA layer, the HA tips rapidly separated from the micropillar base upon skin insertion. Thus, these drugcontaining tips remained implanted into the skin and slowly released their insulin content. Their hypoglycemic effect was demonstrated in vivo in a healthy mouse model.

#### 2.3. Microneedle Patches for Cancer Therapy

Cancer is a life-threatening disease and difficult to cure under current medical technique.<sup>[91]</sup> Conventional therapy includes surgery, chemotherapy, radiotherapy, photodynamic therapy (PDT), photothermal therapy (PTT), and immunotherapy.<sup>[87g,92]</sup> Although those treatments have been improved over the past decades, the effective and targeted delivery of therapeutical agents to the tumor site remains a considerable challenge.<sup>[93]</sup> Skin cancer is a common malignancy in humans and has an

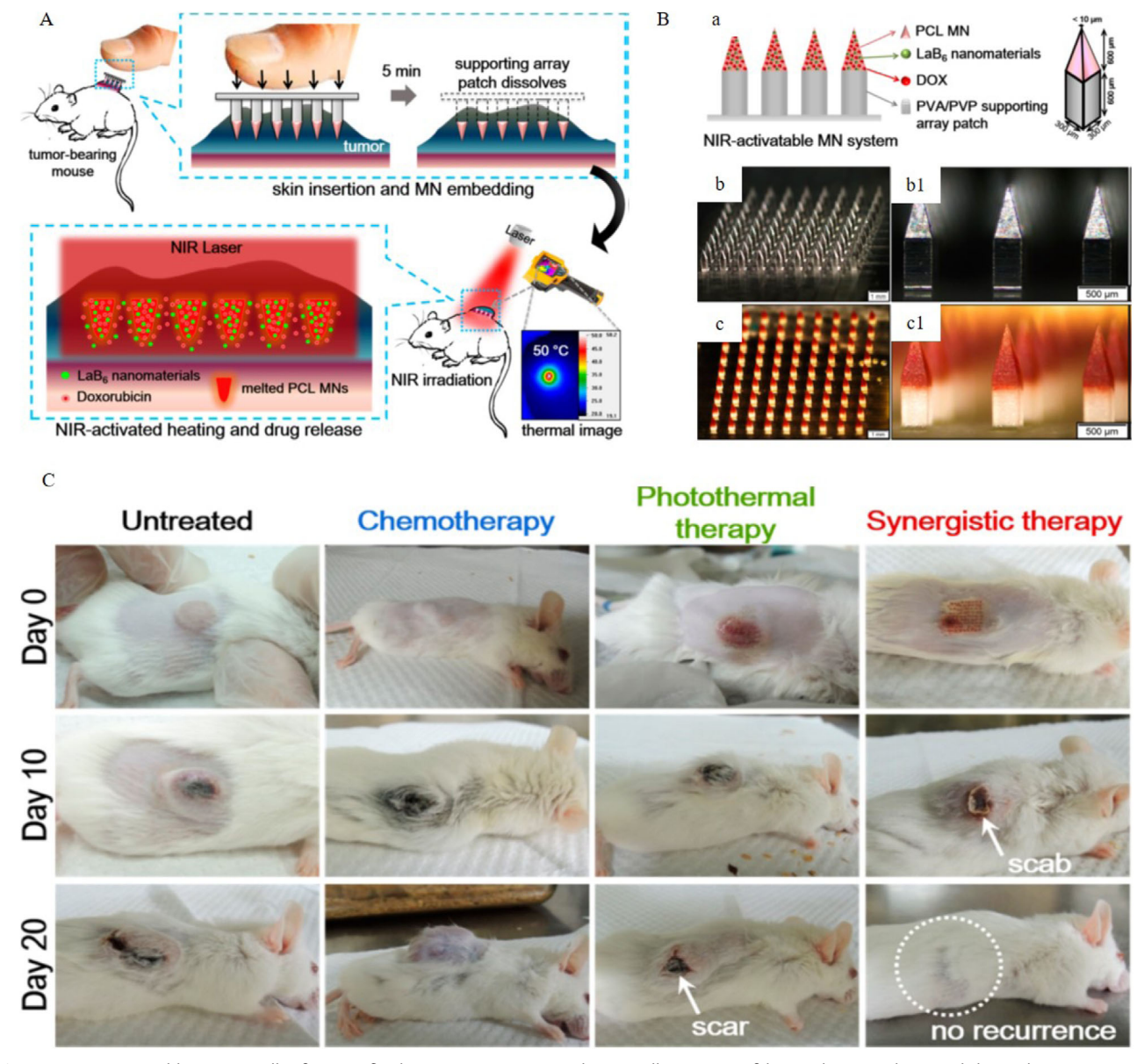


Figure 8. NIR-activatable microneedles for superficial tumor treatment. A) Schematic illustrations of the combinational PTT and chemotherapy treatment by applying a drug-loaded NIR-responsive microneedle patch onto skin tumors. The supporting microneedle array dissolves within 5 min after insertion, leaving the NIR-responsive microneedles inserted under the skin. Upon exposure to NIR light, the photosensitive embedded microneedles can generate localized heat around the tumor area which causes the microneedles to melt, thus releasing the chemotherapy drug. B) Characterization of the NIR light-activatable microneedle patch. The system consists of PVA/PVP dissolving micropillar arrays capped with polycaprolactone microneedles containing photosensitive nanoparticles (lanthanum hexaboride) and an anticancer drug (doxorubicin). a) Schematic representation of the microneedle system together with the microneedle specifications. b,c) Bright-field micrographs of stainless steel microneedle master structure (b, b1) and doxorubicin-loaded polycaprolactone microneedle system (c, c1) (b and c, low magnification; b1 and c, high magnification). C) Photographs of untreated microneedle with doxorubicin intratumorally (chemotherapy), mice treated with microneedles and NIR light (PTT therapy), and mice treated with doxorubicin-loaded microneedles and NIR light (combinational therapy) at days 0, 10, and 20 after treatment. Reproduced with permission. [98] Copyright 2015, American Chemical Society.

increasing incidence.<sup>[94]</sup> For example, it is estimated that one in five Americans will develop skin cancer in their lifetime.<sup>[95]</sup> Particularly, malignant melanoma, that causes millions of deaths every year,<sup>[96]</sup> has high resistance to both radiotherapy and chemotherapy.<sup>[97]</sup> In the recent years, microneedle patches have been developed to target-deliver therapeutic agents into skin tumor sites with high delivery efficacy and reduced side effects.

Microneedles have been employed to deliver anticancer drugs (chemotherapy), as well as PDT and PTT agents, to skin tumor sites in a minimally invasive fashion and with improved therapeutic efficacy. For example, Chen et al. reported NIR light activatable microneedles that are capable to reliably penetrate the skin and simultaneously provide PTT and chemotherapy to combat a skin tumor (Figure 8). [98] Their microneedle patch

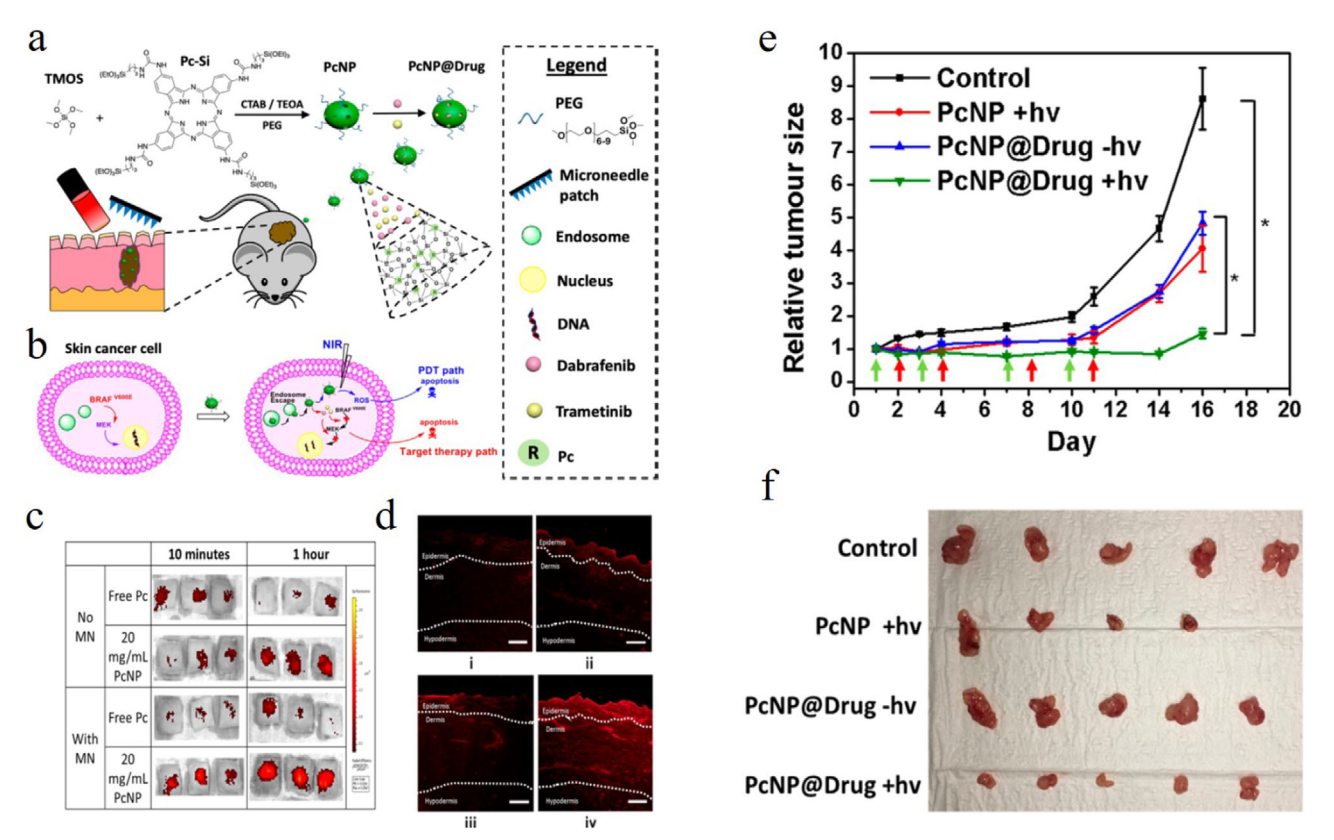


Figure 9. Microneedle-assisted delivery of mesoporous silica nanoparticles for combinational PDT and targeted therapy. a) Schematic of the synthesis of photosensitizer-conjugated and drug-loaded mesoporous silica nanoparticles and its penetration into skin. b) Proposed cellular mechanism for the action of the combinational PDT and targeted therapies based on silica nanoparticles (MN, microneedles; Pc, Phthalocyanine; PcNP, Pc-bonded mesoporous organosilica nanoparticles). c) Fluorescence characterization for the topical penetration of phthalocyanine-conjugated silica nanoparticles (20 mg mL<sup>-1</sup>) versus free phthalocyanine on fresh porcine skin for 10 min and 1 h durations with and without the microneedle assistance. d) Fluorescence imaging of histological sections of porcine skin penetrated with silica nanoparticles (20 mg mL<sup>-1</sup>) for 10 min without microneedles (ii), 10 min with microneedles (iii), 1 h without microneedles (iii), and 1 h with microneedles (iv). Scale bar = 200  $\mu$ m. e) In vivo antitumoral effect of the microneedle-assisted combinational therapy. Relative tumor size growth chart for control, PDT-treated mice in presence of NIR light (PcNP+hv), targeted therapy treated mice without NIR light (PcNP@Drug+hv). The tumor sizes were measured together with the mouse skin using a digital caliper. Green arrow: silica nanoparticle treatment, red arrow: laser treatment. \*p < 0.05, n = 5. f) Photographs of the relative sizes of the excised tumors on day 16 for each group. Reproduced with permission. [99] Copyright 2018, American Chemical Society.

was made of PVA/PVP as a supporting substrate, and embeddable polycaprolactone containing photoresponsive lanthanum hexaboride nanoparticles and an anticancer drug (doxorubicin). This microneedle patch uniformly penetrated into skin and enabled locoregional cancer treatment. Activated by NIR light, the microneedle increased the local temperature up to 50 °C and photothermally ablated the tumor and triggered doxorubicin release. An in vivo mouse xenograft model demonstrated that this microneedle patch completely eradicated a 4T1 tumor within 1 week without observable invasion and side effects.<sup>[98]</sup> Zhao and co-workers synthesized photosensitizer (phthalocyanine) conjugated mesoporous silica nanoparticles co-loaded with two FDAapproved targeted drugs, that is, dabrafenib and trametinib, for combination therapy of mutant melanoma (Figure 9). [99] In vitro tests showed that as-prepared drug free nanovehicles were cytocompatible in contact with normal skin cells in the dark. In contrast, NIR-irradiated drug-loaded nanovehicles showed a synergistic killing effect on skin cancer cells mainly through both reactive oxygen species and caspase-activated apoptosis. [99] In addition, as evaluated using porcine skin, microneedles could facilitate transfer of silica nanoparticles across the epidermis to reach deep-seated melanoma sites. An in vivo study of xenografted melanoma mouse model further confirmed the therapeutic efficacy of the microneedle-assisted delivery of silica nanoparticles for combinational photodynamic and targeted therapy. [99] Apart from those developments, many other studies have been reported that demonstrate the effectiveness and promising future usage of microneedle technique for skin cancer therapy. [100] For instance, Done et al. fabricated Au nanocage-strengthened dissolving microneedles for combined PTT and chemotherapy of skin tumors; [101] Lan et al. reported microneedle-assisted lipid-coated cisplatin nanoparticle cancer therapy; [102] Zhao et al. reported a tip-loaded fast dissolving microneedle patch for PDT. [103]

In addition to cancer chemotherapy, PDT, and PTT, the microneedle patch platform has also been intensively studied for cancer immunotherapy. Cancer immunotherapy that modulate the patient's immune system to identify and kill cancer cells has strong potential for long-term cancer treatment

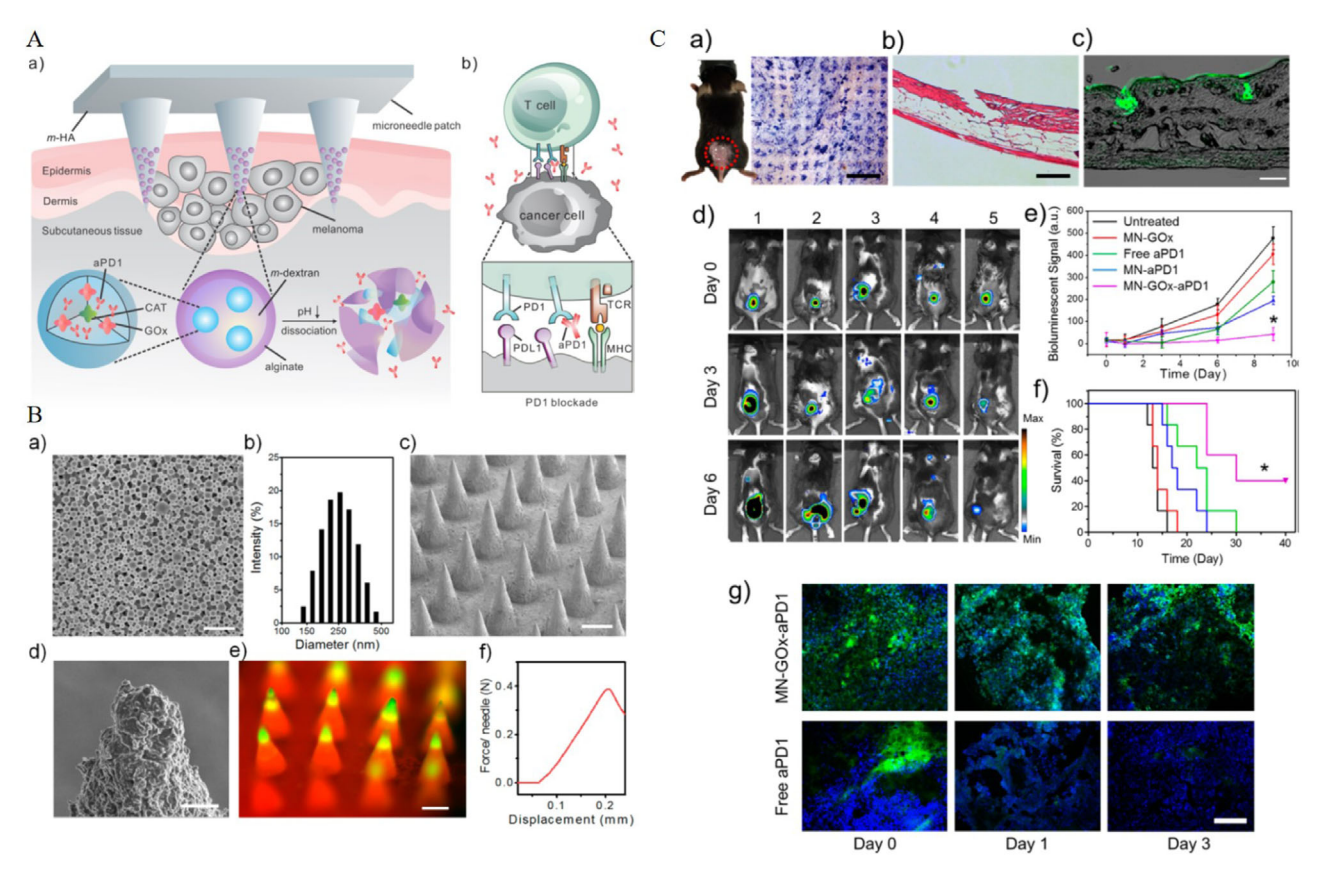


Figure 10. Microneedle patch for skin cancer immunotherapy. A) Schematic of the microneedle-assisted delivery of aPD1 for melanoma treatment. a) Schematic for the delivery mechanism of aPD1 from microneedle arrays containing self-dissociating nanoparticles. b) Schematic of the immunotherapeutic effect of aPD: blockade of PD-1 by aPD1 to activate the immune response and destroy cancer cells. B) Morphological and mechanical characterization of aPD1 loaded microneedles. a) Scanning electron microscopy image of dextran nanoparticles (scale bar: 100 nm). b) The average hydrodynamic sizes of dextran nanoparticles determined by dynamic light scattering. c) Scanning electron microscopy image of microneedle arrays (scale bar: 200 µm). d) High magnification of a microneedle tip by scanning electron microscopy, confirming that the microneedle is composed by nanoparticles (scale bar: 5 µm). e) Fluorescence micrograph of microneedle arrays containing FITC-antibody loaded nanoparticles in their tip (scale bar: 200 µm). f) Mechanical stress characterization for the microneedle patch, showing a failure force of 0.38 N per needle. C) In vivo skin cancer immunotherapy using aPD1-loaded microneedles. a) Mouse dorsum and skin area (marked by a dashed red line) treated with a microneedle patch (left). Optical micrograph of the trypan blue staining displaying penetration of microneedle patch into mouse skin (right) (scale bar: 1 mm). b) Histological hematoxylin and eosin (H&E) stained section of a mouse skin area penetrated by one microneedle (scale bar: 200 µm). c) Merged fluorescence and bright field cross-sectional images of the mouse skin treated with microneedles loaded with FITC-labeled antibodies (green: aPD1) (scale bar: 200 µm). d) In vivo bioluminescence imaging of the B16F10 melanomas for different groups (1, untreated; 2, MN-GO<sub>x</sub>; 3, free aPD1; 4, MN-aPD1; 5, MN-GO<sub>x</sub>aPD1). The error bars represent the standard deviation (SD) of three mice. e) Quantified bioluminescent tumor signals according to (d). f) Kaplan-Meier survival curves for the treated and the control mouse groups (eight mice per treatment group). g) Immunofluorescence staining of tumors treated with MN-GOx-aPD1 or free aPD1 at day 0, day 1, and day 3 (green: aPD1, blue: nucleus) (scale bar:  $100 \mu m$ ). Comparisons of survival curves were made using the log-rank test. \*p < 0.05. Reproduced with permission. [107] Copyright 2016, American Chemical Society.

with reduced risk of cancer metastasis and recurrence.<sup>[104]</sup> Microneedle patches are able to deliver biomolecules to the high density of antigen-presenting cells residing in skin layer, and generate increased antitumor immune response.<sup>[99,105]</sup> For example, programmed death-1 (PD-1) immune checkpoint inhibitors, are FDA-approved negative regulators of tumor-infiltrating lymphocytes and are a very effective weapon to combat various types of cancers and improve patient survival rate.<sup>[106]</sup> Gu and co-workers reported microneedle patch assisted anti-PD1 (aPD1) antibody delivery.<sup>[107]</sup> Their microneedles were composed of biocompatible HA with pH-sensitive dextran nanoparticles loaded with aPD1 and GO<sub>x</sub>. By converting glucose to gluconic acid, the enzyme disrupts dextran nanoparticle structure, resulting in sustained re-

lease of aPD1 (**Figure 10**). In a B16F10 mouse melanoma model, this microneedle patch could generate robust immune responses with a single administration. Besides that, the same group also demonstrate that the microneedle patch is applicable for synergistic immunotherapy with enhanced antitumor immune responses. In [108]

## 2.4. Microneedle Patches for Other Applications

Besides vaccination, diabetes treatment and cancer therapy, the application of microneedle-based systems has also been investigated to successfully treat other diseases or manage skin

conditions. For instance, the usage of microneedle for cosmetic application dates back to early 2000s and has led to the greatest commercial success of the microneedle technique. [109] Microneedles have demonstrated promising results in improving skin appearance and minimizing skin imperfections such as scars, [110] stretch marks, [111] hyperpigmentation, [112] and wrinkles. [113] The large and growing market for cosmetic microneedle products was pioneered by the launch of Dermaroller in 1999 (Wolfenbüttel, Germany), which consists of solid microneedles projecting out from cylindrical rollers.<sup>[109]</sup> By rolling the device on the skin surface, transient micropores are opened. These pores could reach up to the papillary dermis depending on the length of the microneedles (150–1500 µm) and the applied force. [114] Researchers and clinicians have demonstrated that Dermaroller can be used to improve skin texture by reducing fine wrinkles and lines, or even to treat scars and hyperpigmentation.[115] For instance, Dermaroller has been used to treat acne scars by piercing the skin for collagen induction therapy (dermabrasion). Fabbrocini et al. treated human volunteers presenting acne scars with Dermaroller microneedles, observing an overall aesthetic improvement in all patients after only two sessions.<sup>[110]</sup> Dermaroller has also been used in combination with active agents such as glycolic acid for the treatment of acne scars in pigmented skin, with a significant improvement in scar appearance and skin texture, and reduced pigmentation.[115b] Many other companies (e.g., Hansderma, Dermapen) have developed similar products to Dermaroller. Dissolving microneedles have also been used for cosmetic application. Jung and co-workers developed a dissolving HA-based microneedle patch for the delivery of cosmetic products (ascorbic acid and retinyl retinoate).[113] Tests in human volunteers demonstrated improvement of skin appearance by reducing wrinkles and skin roughness. Dissolving microneedle patches have been successfully commercialized for cosmetic purposes. MicroHyala are microneedle patches developed by the pharmaceutical company CosMED (Kyoto, Japan) which are made of dissolving HA and were granted FDA approval in 2004.[116] Upon exposure to the skin moisture, the HA is dissolved and the cosmetic product released.[117] MicroHyala has also been clinically tested for the delivery of influenza vaccines. [118]

Most recently a rapidly separating microneedle patch (where the microneedle tips separate from the supporting substrate) was used for the sustained release of a contraceptive. [119] Sustained-release formulation of contraceptive hormones via self-administration attracts great attention because of its effectiveness, low cost, and convenience. In this study, Prausnitz and co-workers developed biodegradable polylactic acid and polylactic-co-glycolic acid needles for continuous release of the contraceptive hormone levonorgestrel (Figure 11). Bubble structures between the microneedles and the supporting array facilitate the rapid release of the dissolving tips within 5 s after administration. This microneedle patch was tested in rats, revealing that the patch was well tolerated, while maintaining plasma concentrations of the hormone above the therapeutic level for 1 month. [119]

Water-soluble microneedles are well suited for skin delivery, since aqueous contact does not occur on the most external layers of the skin, thus preventing dissolution prior to penetration. However, for wet tissues, such as buccal, ocular and mucosal routes, the dissolving speed must be slowed down to prevent

microneedle dissolution before penetration into the tissue. Than et al. reported self-implantable double-layered microdrug-reservoirs for efficient and controlled ocular drug delivery (Figure 12).[120] Fast dissolving HA was covered by slow dissolving crosslinked methacrylated HA (MeHA) to slow down dissolution, facilitating penetration of the wet cornea surface before loss of mechanical strength. In a corneal neovascularization disease model, the delivery of an anti-angiogenic monoclonal antibody (DC101) produced approximately 90% reduction of neovascular area with minimal invasion.[120] Gu et al. reported a feedback-controlled anticoagulant system based on thrombinresponsive polymer-drug conjugates for auto-anticoagulant regulation (Figure 13).[121] Thrombin-responsive heparin (HP) conjugated HA was fabricated by using a thrombin-cleavable peptide as a linker to conjugate HP to the main chain of HA. The fabricated thrombin-responsive HP conjugated HA (TR-HAHP) was used to generate a microneedle patch for transcutaneous delivery. Triggered release of the HP from microneedle patch was achieved upon exceeding a threshold thrombin concentration, reducing risk of over- or under-dosage. In addition, in vivo study in thrombolytic challenge model demonstrated long-term effectiveness.[121]

Microneedle patches have also been applied for the treatment of bacterial infections.[122] The microneedle-assisted local delivery of antimicrobial agents have shown enhanced therapeutic effects for epidermal wounds<sup>[122b]</sup> as well as for subcutaneous infections. [122c] Recently, Chen and co-workers have developed dissolving microneedle patches composed of an antifugal and antibacterial chitosan-polyethylenimine copolymer.[122c] Dissolving antibacterial polymers, apart from enabling sustained release, also have the advantage of not inducing drug resistance as they act by physically disrupting microbial membranes.[122c] The antibacterial effect of this copolymer was proven to last for up seven days. Additionally, the authors showed that antimicrobial drugs such as amphotericin B can be loaded in the copolymer matrix, and that the codelivery of both active agents provides enhanced therapeutic effects against subcutaneous fungal infection. In vivo experiments showed that the local, sustained delivery facilitated by these patches provides a superior antimicrobial effect when compared to topical drug delivery.

Microneedle patches are also utilized for many other disease treatments or biomedical applications, such as hair regrowth,<sup>[123]</sup> analgesia,<sup>[87a,124]</sup> acute migraine,<sup>[125]</sup> and obesity.<sup>[126]</sup>

# 3. Nanoparticles for Transdermal Delivery

In this section, we review the most recent efforts to design and develop nanoparticles and nanoscaled systems for enhanced transdermal delivery.  $^{[127]}$ 

For the past decade, nanotechnology has improved therapeutics in a number of medical fields, including cancer, wound healing, and cardiology. Drug nanocarriers have been designed in various architectures, ranging from nanoparticles (0D), nanowires, and nanotubes (1D), nanosheets (2D) to 3D architectured nanomaterials. One of the major advantages of nanomaterials is that they can be engineered for specific functionalities, such as sustained/triggered release, increased stability and solubility, targeted delivery to specific sites, and

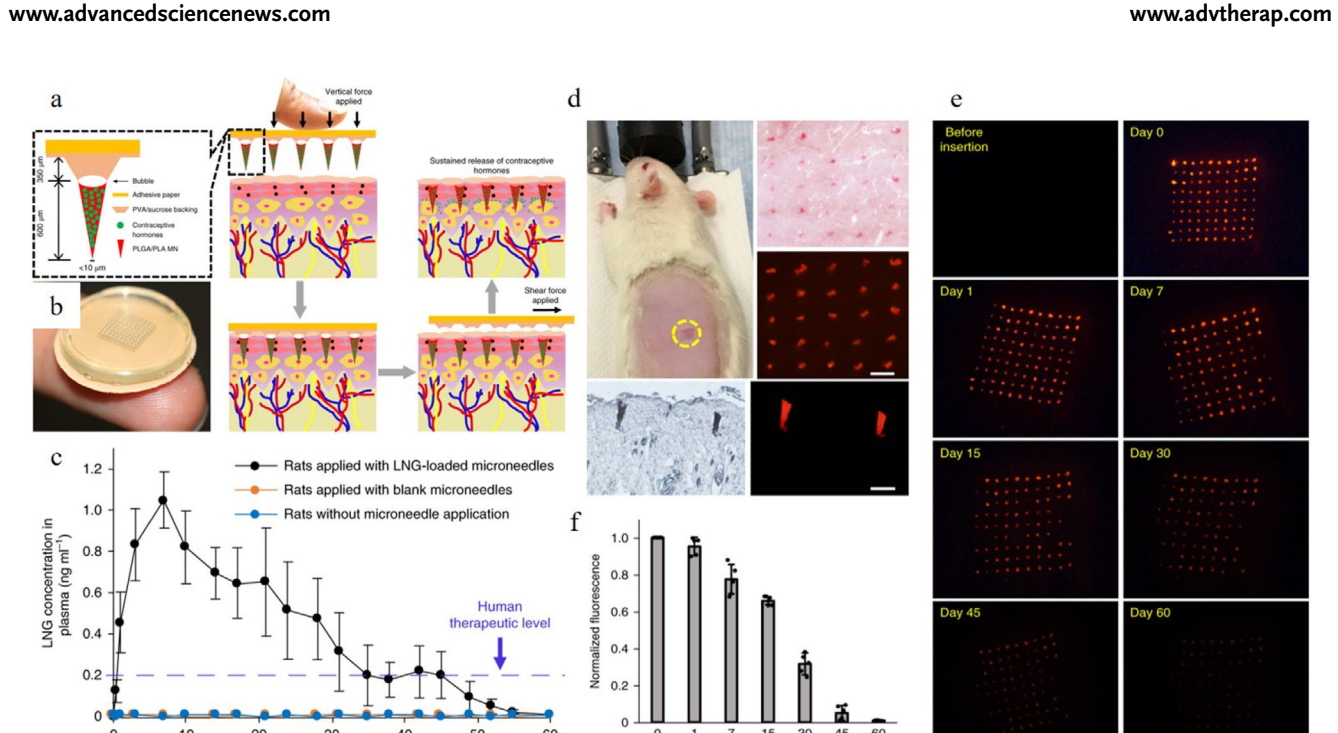


Figure 11. Rapidly separating microneedle patches for the sustained release of a contraceptive. a,b) Design and application of rapidly separating microneedle patches. a) Left and inset, schematic representation of the microneedle design containing a bubble that enables rapid separation from the supporting substrate. Right, illustration of the microneedle patch application using first a vertical force to pierce the skin, then and a shearing force to detach the supporting substrate. b) Photograph of the patch containing 100 individual microneedles. c) Rat plasma concentrations of the contraceptive monitored for up to 60 h after administration of levonorgestrel-loaded microneedle patches, where the dashed blue line indicates the human therapeutic levonorgestrel level. Rats administered with blank microneedle patches and untreated rats were used as controls. d-f) Characterization of dye release from rapidly separating microneedle patches applied in vivo in rats. d) Top left, photograph of the rat dorsum after application of Nile red-loaded microneedles, with the application area delimited with a yellow dashed circle. Bright-field (top right) and fluorescence microscopy (middle right) micrographs of the skin after microneedle patch application and removal, where the red dot arrays correspond to microneedles embedded in the skin. Scale bar, 500 µm. Histological sections of rat skin images by bright-field (bottom left) and fluorescence (bottom right) microscopy, displaying the microneedles embedded into the skin. Scale bar, 200 µm. e) Fluorescence images of the skin surface before and after insertion of a Nile red-loaded microneedle patch into rat skin in vivo at different time points (days 0, 1, 7, 15, 30, 45, and 60), illustrating the dye release during microneedle degradation. Scale bar, 2 mm. f) Quantitative analysis of the skin fluorescence intensity after administration of a Nile red-loaded microneedle patch at different time points (days 0, 1, 7, 15, 30, 45, and 60). Data are normalized to day 0. Bars represent means  $\pm$  SD (n = 5 independent animals). Reproduced with permission.[119] Copyright 2019, Springer Nature.

enhanced permeation and retention (EPR).[130] Nanosystems can selectively interact with different biological entities (such as DNA, RNA, and proteins) by carefully controlling the properties of the nanomaterial (e.g., size, surface chemistry, morphology, and chemical composition).[131]

Encouraged by the success that therapeutic nanotechnological approaches have achieved in other medical fields, nanomaterials have increasingly been investigated for transdermal drug delivery. Nanoparticles may be employed to enhance the transport of active agents through the stratum corneum and into the viable layers of the skin. They may be also used to facilitate the drug penetration into the skin by increasing aqueous solubility.[132] In addition, nanoparticulate systems can be further functionalized with targeting ligands to achieve targeted release within the skin.

There are two possible transdermal transport routes for nanocarriers: i) along skin appendages including hair follicles, pilosebaceous pores, and sweat gland pore (Figure 14A); or ii) through the intercellular routes that exist between corneocytes and along the lipid matrix (Figure 14B). [132] Polymeric nanoparticles, nanoemulsions, solid liposomes, metal/metal oxide nanostructures and dendrimers are the most commonly used nanocarriers for transdermal delivery. [133] These nanoparticles are typically regarded as cost-effective and safe, and also possess high drug-loading capacity. Indeed, since Doxil (a liposomal nanoformulation) was approved in 1995, more than 50 nanocarriers have received FDA approval and are available for clinical use. [134] Most typically, these are administered via intravenous injection and, less frequently, transdermally. The skin permeation of these nanocarriers is strongly limited by their size. Recent reports have shown that solid nanoparticles between 10 and 100 nm in size penetrate poorly into human skin. [135] This has encouraged extensive investigations in engineering the shape, chemistry, and deformability of nanocarriers from the perspective of understanding the mechanisms involved in the nanoparticle transport through the skin. This essential research has led to the successful application of nanoparticle systems for transdermal drug delivery for a variety of conditions, including enhanced vaccination, treatment of skin cancer, infection and chronic wounds, and diabetes.[136]

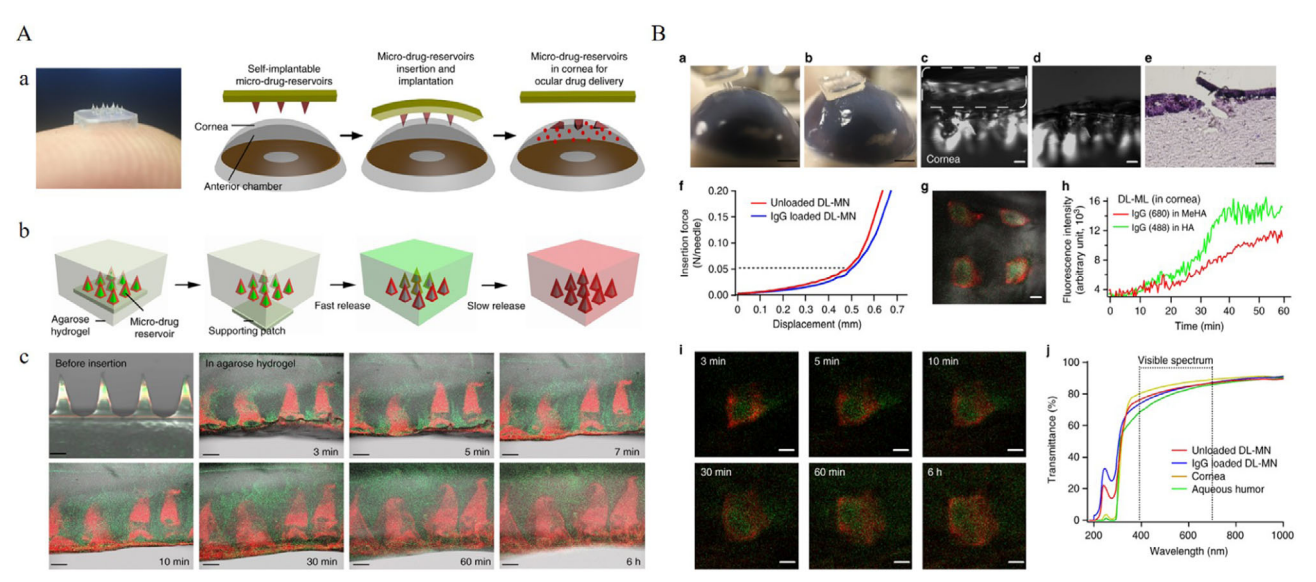


Figure 12. Self-implantable double-layered microneedles for ocular drug delivery. A) Schematic illustrations and in vitro characterization of the biphasic release from double-layered microneedles. a) Photograph of the microneedle patch resting on a finger (left) and schematic illustration of the eye-contact patch for ocular delivery. b) Schematic showing the biphasic release profile from double-layered micro-drug-reservoirs, with fast release represented in green and slow release in red. c) The merged (optical and fluorescent) images of double-layered microneedles before insertion and after insertion in agarose hydrogels, showing real-time release of IgG (680) (red color) and IgG (488) (green color) at different time points (from 3 min to 6 h). Scale bars: 200  $\mu$ m. B) Ex vivo evaluation of double-layered microneedles for ocular delivery. Bright-field images of the cornea before (a) and after (b) microneedle application. Scale bars: 2 mm. Cross-sectional image of the cornea after microneedle application (c) and after removal of the supporting patch (d). Scale bars: 200  $\mu$ m. e) Hematoxylin and eosin (H&E) stained section of the cornea after microneedles penetration. Scale bar: 100  $\mu$ m. f) The force applied to double-layered microneedles (n = 3). g) Confocal image of cornea after double-layered microneedles applied, h) fluorescence intensity increased (n = 4) in the region adjacent to double-layered microneedles, and i) confocal images of IgG (680) (red color) and IgG (488) (green color) in the cornea. Scale bars: 100  $\mu$ m. j) Transmittance of the fully-hydrated double-layered microneedle, cornea and aqueous humor (n = 3). Reproduced with permission. [120] Copyright 2018, Springer Nature.

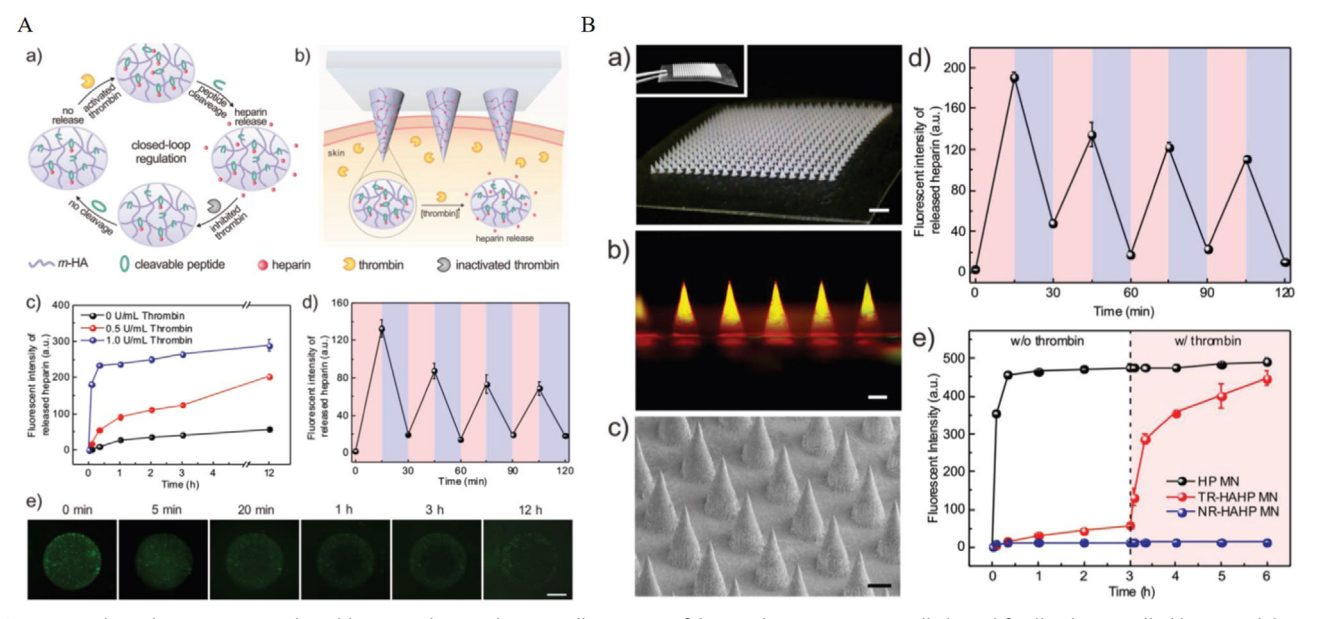


Figure 13. Thrombin-responsive closed-loop patch. A) Schematic illustration of the mechanism microneedle based feedback-controlled heparin delivery (a, b). c) Accumulated FITC-labeled HP release in response to different thrombin concentrations at 37 °C. d) Pulsatile release profile of FITC-HP from the TR-HAHP hydrogel (blue indicates without thrombin; pink indicates with thrombin). e) Fluorescent images of the TR-HAHP hydrogel in thrombin solution at different time points. Scale bar = 1 mm. B) Fabrication and in vitro characterization of the thrombin-responsive patch. a) Photographs of the microneedle patch. Scale bar: 1 mm. b) A fluorescence image of rhodamine-labeled microneedles loaded with FITC-labeled TR-HAHP. Scale bar: 200 μm. c) A scanning electron microscopy image of microneedle arrays. Scale bar: 200 μm. d) Pulsatile release profile of FITC-HP from the TR-HAHP microneedle patch (blue indicates without thrombin; pink indicates with thrombin). e) FITC-HP release from microneedle patch in response to thrombin solutions. Reproduced with permission. [121] Copyright 2017, Wiley-VCH.

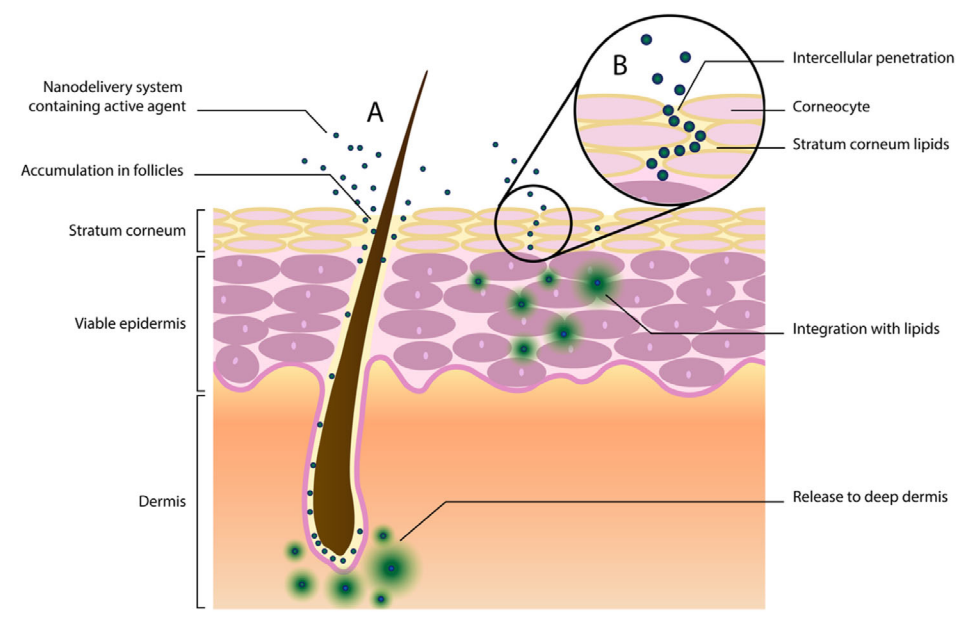


Figure 14. Structure of skin revealing routes of nanoparticle penetration through A) skin appendages including hair follicles, pilosebaceous pores, and sweat gland pores; and B) through the intercellular routes.

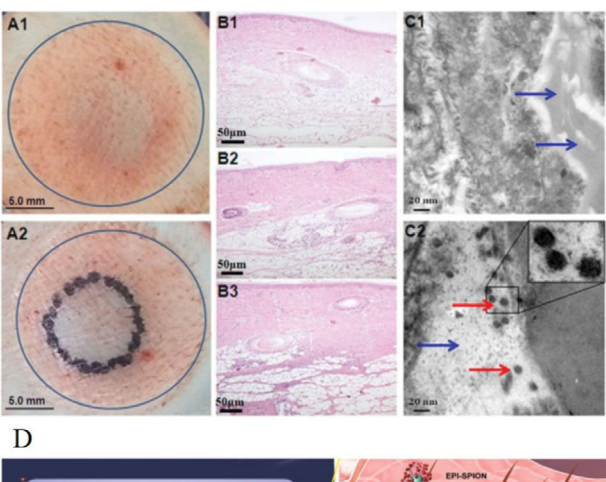
# 3.1. Treatment of Skin Cancer

Many nanocarriers have been designed and synthesized for application in improved treatments of skin cancer, which is one of the most common skin malignancies. [100c,137] Nanoparticles can be engineered to locally deliver anti-cancer drugs to the tumor site thus improving treatment efficacy and reduce side-effects. For example, Rao et al. reported that superparamagnetic ironoxide nanoparticles (SPIONs), loaded with the model anticancer agent epirubicin (EPI), could circumvent the stratum corneum via the follicular route for enhanced skin cancer treatment.[138] In this nanosystem, EPI was covalently conjugated to SPIONs and driven by an external magnetic field to deeper regions of the skin. This magnetic field assisted SPIONs transdermal delivery system actively inhibited melanoma WM266 cell proliferation in a dose-dependent way. In addition, in vitro transdermal studies revealed that SPIONs were able to penetrate deep inside the skin with the help of an external magnetic field as shown in Figure 15.[138] Wiraj et al. applied framework nucleic acid (FNAs) nanostructures for transdermal delivery and melanoma treatment with minimal skin disruption.<sup>[139]</sup> FNAs with different shapes and sizes were evaluated for their ability to penetrate in mice and human skin explant. A size-dependent penetration was found: FNAs ≤75 nm could effectively reach dermis, with 17 nm FNAs exhibiting the best penetration to up to 350 µm depth. Moreover, in vivo mouse melanoma model studies showed that doxorubicin-loaded FNAs gave a twofold enhancement of drug accumulation and tumor inhibition compared to doxorubicin-loaded liposomes or polymeric nanoparticles. [139]

#### 3.2. Treatment of Infection

Chronic skin wounds are commonly accompanied by bacterial infection, and the treatment of the infection is essential to avoid

wound aggravation.[136e,140] Despite the availability of a range of antibiotics, morbidity and mortality of chronic wound patients remain high because of the growing number of multidrug resistant microorganisms.[141] Therefore, there is a crucial need to develop new strategies to combat chronic skin wound infection and improve wound healing. For this purpose, the use of nanodelivery systems appears in a privileged position due to their versatility, cost-effectiveness, safety, and effectiveness. Indeed, a range of nanoparticles have been proposed for enhanced wound healing in recent times. The most common candidates as antibacterial agents are silver nanoparticles which are effective against both gram-positive and gramnegative bacteria.[142] Besides silver, many other nanoparticles have been designed to treat wound infection. For example, porous silicon has been designed to combat bacteria and microbial infection.<sup>[143]</sup> In one study, Alhmoud et al. fabricated gold nanoparticles decorated porous silicon nanopillars for targeted hyperthermal treatment of bacteria.[144] In this study, the nanocomposites could be activated by NIR laser irradiation and inhibit the growth of *Staphylococcus aureus*.<sup>[144]</sup> Functional metalorganic framework nanoparticles have been also fabricated for skin infection treatment. Light-responsive zeolitic imidazolate framework (ZIF) nanoparticles were fabricated as rifampicin nanocarriers (Figure 16). [145b] In this study, ZIF was formulated with 2-nitrobenzaldehyde (o-NBA) to act as a light responsive nanocarrier. Upon light irradiation, 2-nitrobenzaldehyde could lower pH and trigger degradation of ZIF nanoparticles, thus controlling the release of the antibiotic rifampicin (RFP). In addition, the dissolution of scaffolding ZIF nanoparticles resulted in the release of Zn<sup>2+</sup> ions, giving an additional curative effect.<sup>[145b]</sup> 2D materials have been also synthesized for skin bacterial disinfection and wound healing applications.<sup>[146]</sup> As an example, Li et al. reported using Zn2+ and graphene oxide modified g-C<sub>3</sub>N<sub>4</sub> to promote wound healing and kill bacteria at the same time by short-time exposure to 660 and 808 nm light.[147]



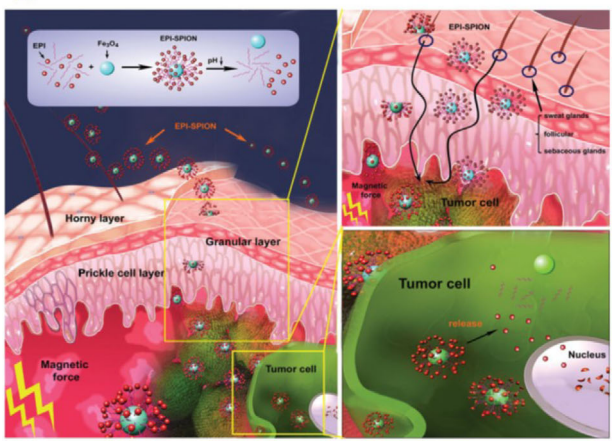


**Figure 15.** EPI-loaded SPION for transdermal delivery. A–C) Evaluation of magnetic transdermal delivery of EPI–SPION particles via modified Franz's cell method. A) EPI–SPION particles distribution on the skin is shown in the absence (A1) and presence (A2) of an external permanent ferromagnet. B) H&E stained histological section. Control (B1) and EPI–SPION (B2, B3). C) TEM images of skin section, where blue arrows indicate the pilosebaceous unit and red arrows indicate EPI–SPION particles. D) Schematic illustration of EPI-loaded SPION for magnetic transdermal delivery against skin cancers. Reproduced with permission. [138] Copyright 2015, Wiley-VCH.

Zn<sup>2+</sup> and graphene modified g-C<sub>3</sub>N<sub>4</sub> generated a photodynamic and photothermal antibacterial effect upon co-irradiation, which killed over 99.1% of *S. aureus* and *Escherichia coli*. In addition, Zn<sup>2+</sup> and graphene oxide upregulated the expressions of matrix metalloproteinase-2 (MMP-2), type III collagen (COL-III), and type I collagen (COL-I), which accelerated wound healing. [147] Many other nanomaterials have been reported for skin infection treatment and enhanced wound healing, including metal nanoparticles, [148] polymeric nanoparticles, [149] nanogels, [150] copper sulphide nanoparticles, [151] zinc oxide nanoparticles, [152] porous silicon nanoparticles, [153] etc.

## 3.3. Other Applications

Nanocarriers have also been utilized for other therapeutic applications. For example, Zhang et al. prepared 5-aminolevulinic acid loaded nanoethosome gels for transdermal delivery in the treat-

ment of hypertrophic scars.<sup>[154]</sup> Hypertrophic scars are caused by persistent dermal fibrosis, irregular collagen deposition, and overproliferative hypertrophic scar fibroblast.[155] In this study. nanoethosomes were demonstrated to penetrate the skin barrier and deliver a higher dose of 5-aminolevulinic acid into human hypertrophic scars in vitro. In vivo evaluation in rabbit hypertrophic scars model revealed that nanoethosomes facilitated transdermal delivery of 5-aminolevulinic acid, and improved PDT for hypertrophic scars.[154] Yang et al. examined liposome encapsulated X<sub>I</sub>-DNA to alleviate atopic dermatitis symptoms.<sup>[156]</sup> X<sub>I</sub>-DNA are X-shaped double-stranded oligonucleotides that can induce activation of innate immune cells.<sup>[157]</sup> Confocal microscopy demonstrates that this nanostructure can efficiently penetrate into the epidermis and dermis, and alleviate atopic dermatitis symptoms in mice.[157] In addition, nanoparticles have also been utilized for improved vaccination. For example, Li et al. demonstrate that aluminum hydroxide nanoparticles exhibited higher vaccine adjuvant activity than traditional aluminum hydroxide microparticles.[136b] In this experiment, ovalbumin and Bacillus anthracis protective antigen protein was used as model antigens. Aluminum hydroxide nanoparticles of 112 nm diameter induced a stronger antigen-specific antibody response than 9.3 um aluminum hydroxide microparticles. More recently, Chen et al. reported on a clay nanoparticle (layered double hydroxides or hectorite)-based vaccine formulation that was loaded with three recombinant antigens (intimin  $\beta$ , proprietary antigen 1 and proprietary antigen 2) for the control of pathogenic E. coli.[136c] This study shows that clay nanoparticles generated significantly higher immune responses compared to a commercial adjuvant QuilA formulation.

# 4. Biointegrated Functional On-Skin Devices

Wearable biointegrated functional devices that are capable to noninvasively monitor biological activities, store and analyze data, and deliver therapeutics via a feedback loop, are very promising for personalized medicine and healthcare applications. [158] Such devices promise to improve management of high incidence diseases, such as heart failure, diabetes, and Parkinson's disease. [159]

In recent years, there have been some key advances in the development of wearable biointegrated functional on-skin devices.<sup>[73,160]</sup> For example, Kim and co-workers fabricated a multifunctional, skin-wearable device that integrated stretchable temperature and strain sensors, a non-volatile memory, and a thermal drug release actuator (Figure 17A).[158] This wearable patch was able to monitor motion-related neurological disorders, and controllably deliver drugs via the diagnostic feedback. In this study, Parkinson's was used as model disease to demonstrate how this system works: first, movement disorders were measured by the strain sensor and the data were stored in an integrated memory device; second, collected data were analyzed and, depending on the feedback, transdermal delivery (drug released from mesoporous-silica nanoparticles) was triggered and controlled by thermal stimuli (heat) (Figure 17A). [158] In addition, the same group further developed a graphene-based electrochemical device with thermo-responsive microneedles for sweat-based diabetes monitoring and feedback-controlled transdermal delivery

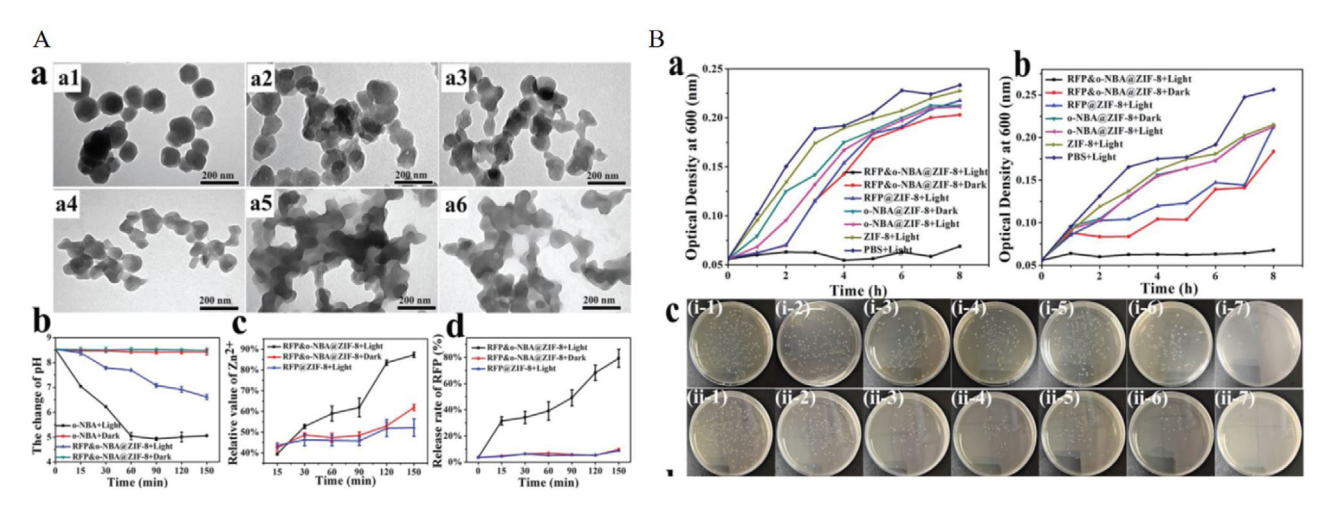


Figure 16. Light-responsive (ZIF) nanoparticles as rifampicin nanocarriers for treatment of bacterial infections. A) Morphological and in vitro characterization of the light-responsive ZIF nanoparticles. a) TEM of RFP&o-NBA@ZIF-8 treated with UV irradiation for different periods of time (a1–a6: 15, 30, 60, 90, 120, 150 min). b) pH change; c) the release efficiency of Zn2+, and d) the antibiotic release efficiency after UV light treatment for different periods of time. B) The optical density at 600 nm (OD600) of ampicillin-resistant *Escherichia coli* (a) and MRSA (b) after treatment with 10 μg mL<sup>-1</sup> of materials under different conditions. c) Coated flat panel of i) Ampicillin-resistant *E. coli* and ii) MRSA treated under different conditions: 1) PBS + Light, 2) ZIF-8 + Light, 3) o-NBA@ZIF-8 + Dark, 4) o-NBA@ZIF-8 + Light, 5) RFP@ZIF-8 + Light, 6) RFP&o-NBA@ZIF-8 + Dark, and 7) RFP&o-NBA@ZIF-8 + Light. Reproduced with permission. [145b] Copyright 2018, Wiley-VCH.

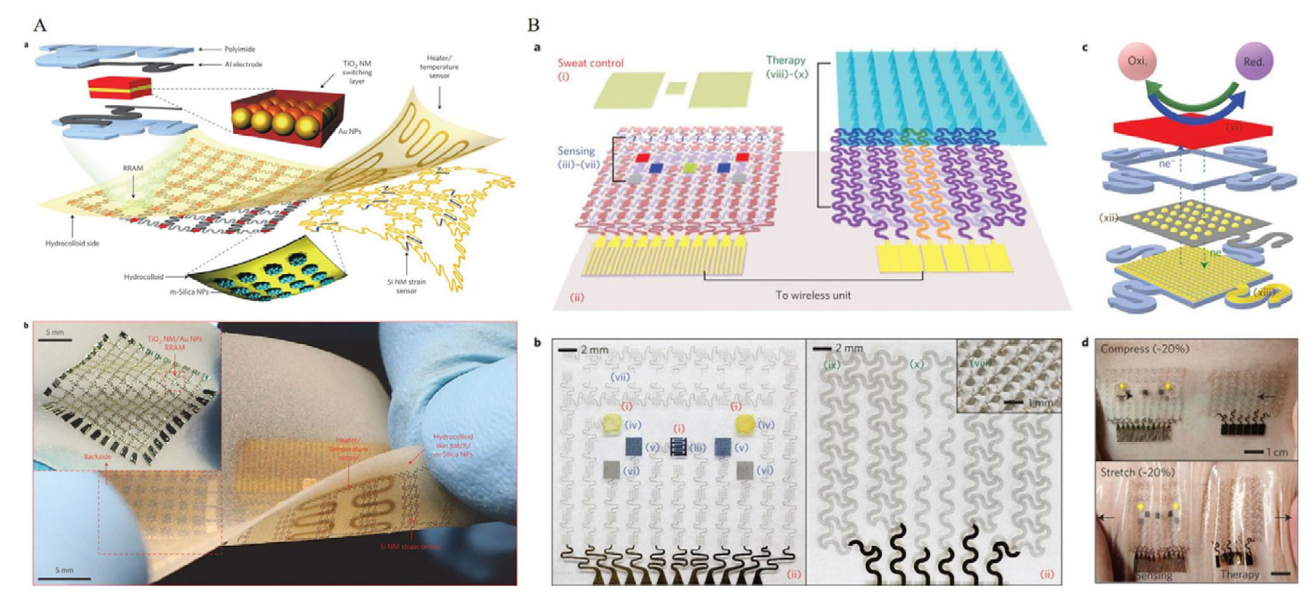


Figure 17. A) Schematic illustration of wearable electronic patch. a) Wearable memory array that consists of a TiO<sub>2</sub> NM–Au NPs–TiO<sub>2</sub> NM switching layer and Al electrodes. On the top-side of the patch, the electroresistive heater/temperature sensor was fabricated, with the Si strain sensor on the opposite side. b) Digital image of wearable electronic patch, showing the wearable bio-integrated system. Reproduced with permission. [158] Copyright 2014, Macmillan Publishers. B) Schematic illustration of the graphene-hybrid electrochemical devices and thermoresponsive drug delivery microneedles. a) Components of the diabetes patch: the sweat-control (i, ii), sensing (iii–vii) and therapy (viii–x). b) Optical images of the electrochemical sensor array (left), therapeutic array (right) and microneedles (inset). Components include: i) sweat-uptake layer (Nafion); ii) water-proof film (silicone); iii) humidity sensor; iv) glucose sensor; v) pH sensor; vi) counter electrode (Ag/AgCl); vii) tremor sensor (graphene); viii) microneedles with drugs (PVP loaded with metformin); ix) heater (gold mesh/graphene); x) temperature sensor (graphene). c) Schematic illustration of the graphene-hybrid electrochemical unit: electrochemically active and soft functional materials xi), gold-doped graphene xii) and a serpentine Au mesh xiii). d) Optical images of the diabetes patch on human skin. Reproduced with permission. [43] Copyright 2016, Macmillan Publishers.

of hypoglycemic drug (metformin).<sup>[43]</sup> The system consists of a heater, sensors (temperature, humidity, glucose, and pH), and polymeric microneedles. Figure 17B illustrates how the system is integrated. In response to a signal from the sensors, polymeric microneedles were thermally triggered (by heat) to deliver metformin and reduce blood glucose levels in diabetic mice.

# 5. Conclusion, Perspectives, and Future Outlook

The transdermal delivery route is attracting increasing attention for treating not only skin diseases but also systemic conditions. Minimal pain and discomfort, bypassing first-pass effects and enzymatic degradation, and diminished systemic toxicity are merits that make transdermal delivery promising for clinical translation. This article provides a comprehensive review about recent development in microneedles and nanocarriers for transdermal delivery. Generally, both techniques are fast growing from a fancy concept to a well-developed research field because of their cost-effectiveness, ease of administration and high efficacy. A broad range of drugs, proteins, biomolecules have been successfully delivered using these systems in vitro and in vivo.

From a microneedle patch aspect, whereas a number of solid non-dissolving microneedle devices are already well established marketed products (e.g., Dermaroller, Dermapen) with high consumer acceptance, especially for cosmetic applications, current research focus is shifting toward polymeric dissolving and biodegradable microneedles for systemic disease treatment. Nowadays, the design purpose of microneedle arrays is not simply to enhance the transdermal delivery efficacy, but also to respond to the biological environment and achieve controlled release. In addition, another focus of microneedle patches is on the translation of transdermal delivery approaches into clinical practice. Indeed, there are approximately 23 active and 39 completed National Institutes of Health (NIH) clinical trials relating to microneedle techniques.[130f,161] Most clinical trials are currently using solid non-dissolving microneedle systems, with a few cases using dissolving microneedles. For example, very recently a solid microneedle patch consisting of a rectangular array of 351 pyramidal, 700 µm long microneedles (Microchannel Skin System by 3M Company) for transdermal delivery of aminolevulinic acid successfully passed a Phase I study (ClinicalTrials. gov Identifier: NCT01812837). Likewise, safety, immunogenicity, and acceptability of dissolving microneedle patch vaccination against influenza were demonstrated in a completed Phase I study (ClinicalTrials.gov Identifier: NCT02438423).[163] Although extensive research has been carried out and successfully demonstrated transdermal delivery efficacy using the microneedle technique, several challenges remain. For example, the choice of appropriate biocompatible biomaterials that allows high mechanical strength, high stability, and suitable drug loading-capacity is still limited. This issue may be addressed by modifying existing biomaterials or exploring newly synthesized biomaterials that are suitable to fabricate microneedle patches. The rapidly progressing field of nanotechnology will most likely be playing a central role in the advancement of microneedle-assisted transdermal delivery. In addition, further investigations on the long-term toxicity of the newest materials continue to be necessary to demonstrate their biocompatibility and biosafety. Also, the challenge of upscaling the microneedle patch fabrication in a cost-effective way remains. Polymer microneedle patches fabricated via molding approaches may be more cost-effective than silicon or metal microneedle patches. Research commercialization is another challenge at current stage. Although dramatic advances have occurred in the last few years, there are competing requirements for the academic research and the industrial research community: academic research is currently primarily focused on flexibility in microneedle patch fabrication whereas industry prioritizes cost-effectiveness and reliability. In the near future, the scientific community may need to find a balance. For accelerating the access of this technology to patients, the robust scientific foundations need to be combined with strong commercialization schemes.

From a nanoparticle transdermal delivery perspective, it has already been demonstrated that nanoparticles have the potential to effectively deliver drugs across the skin. However, the clinical studies of nano-based delivery systems for transdermal delivery are rare. As an illustrative example, a Phase I study (ClinicalTrials.gov Identifier: NCT02467673) evaluated nanoparticle-based formulation of progesterone (10%) combined with estriol (0.1%) + estradiol (0.25%) for transdermal hormone therapy. For successful translation of this promising technology, it is critically important to evaluate the transdermal delivery efficacy and penetration depth of nanoparticles of different morphology, size, and composition as well as establish long-term safety profiles for nanoparticles toward skin and the whole body.

# **Acknowledgements**

L.Y. and M.A. contributed equally to this work. This work was performed in part at the Melbourne Centre for Nanofabrication (MCN) in the Victorian Node of the Australian National Fabrication Facility (ANFF). M.A. gratefully acknowledges the National Health and Medical Research Council (NHMRC) of Australia (GNT1125400). Funding from the Probing Biosystems Future Science Platform of the Commonwealth Scientific and Industrial Research Organisation of Australia (CSIRO) is also kindly acknowledged.

## **Conflict of Interest**

The authors declare no conflict of interest.

## **Keywords**

microneedles, nanomaterials, nanoparticles, transdermal delivery

Received: July 17, 2019 Revised: September 5, 2019 Published online: September 25, 2019

<sup>[1]</sup> C. A. Lipinski, Drug Discovery Today: Technol. 2004, 1, 337.

<sup>[2]</sup> a) V. K. Rai, N. Mishra, K. S. Yadav, N. P. Yadav, J. Controlled Release 2018, 270, 203; b) M. R. Prausnitz, Adv. Drug Delivery Rev. 2004, 56, 581; c) Y. J. Li, J. Y. Wu, X. B. Hu, J. M. Wang, D. X. Xiang, Nanomedicine 2019, 14, 493; d) M. Sheikhpour, L. Barani, A. Kasaeian, J. Controlled Release 2017, 253, 97; e) A. George, P. A. Shah, P. S. Shrivastav, Int. J. Pharm. 2019, 561, 244.

- [3] a) F. Pastorino, C. Brignole, D. Di Paolo, P. Perri, F. Curnis, A. Corti, M. Ponzoni, Small 2019, 15, 1804591; b) H. J. Zhu, J. X. An, C. C. Pang, S. Chen, W. Li, J. B. Liu, Q. X. Chen, H. Gao, J. Mater. Chem. B 2019, 7, 384; c) M. R. Yu, L. Xu, F. L. Tian, Q. Su, N. Zheng, Y. W. Yang, J. L. Wang, A. H. Wang, C. L. Zhu, S. Y. Guo, X. X. Zhang, Y. Gan, X. F. Shi, H. J. Gao, Nat. Commun. 2018, 9, 2607; d) J. Yan, W. X. He, S. Q. Yan, F. Niu, T. Y. Liu, B. H. Ma, Y. P. Shao, Y. W. Yan, G. Yang, W. Y. Lu, Y. P. Du, B. Lei, P. X. Ma, ACS Nano 2018, 12, 2017; e) S. H. Kang, S. J. Hong, Y. K. Lee, S. Cho, Polymers 2018, 10, 948.
- [4] a) L. Wang, M. Zheng, Z. G. Xie, J. Mater. Chem. B 2018, 6, 707; b)
   O. S. Fenton, K. N. Olafson, P. S. Pillai, M. J. Mitchell, R. Langer, Adv. Mater. 2018, 30, 1705328.
- [5] A. Mullard, Nat. Rev. Drug Discovery 2019, 18, 85.
- [6] a) M. R. Prausnitz, R. Langer, Nat. Biotechnol. 2008, 26, 1261; b) G. Yang, Q. Chen, D. Wen, Z. Chen, J. Wang, G. Chen, Z. Wang, X. Zhang, Y. Zhang, Q. Hu, L. Zhang, Z. Gu. ACS Nano 2019, 13, 4354; c) J. Wang, J. Yu, Y. Zhang, X. Zhang, A.R. Kahkoska, G. Chen, Z. Wang, W. Sun, L. Cai, Z. Chen, C. Qian, Q. Shen, A. Khademhosseini, J.B. Buse, Z. Gu. Sci. Adv. 2019, 5, eaaw4357.
- [7] X. Chen, Adv. Drug Delivery Rev. 2018, 127, 85.
- [8] a) H. Lee, C. Song, S. Baik, D. Kim, T. Hyeon, D. H. Kim, Adv. Drug Delivery Rev. 2018, 127, 35; b) P. C. Pandey, S. Shukla, S. A. Skoog, R. D. Boehm, R. J. Narayan, Sensors 2019, 19, 1028; c) O. A. Al Hanbali, H. M. S. Khan, M. Sarfraz, M. Arafat, S. Ijaz, A. Hameed, Acta Pharm. 2019, 69, 197.
- [9] a) J. O. Morales, K. R. Fathe, A. Brunaugh, S. Ferrati, S. Li, M. Montenegro-Nicolini, Z. Mousavikhamene, J. T. McConville, M. R. Prausnitz, H. D. C. Smyth, AAPS J. 2017, 19, 652; b) B. A. Curikova, K. Prochazkova, B. Filkova, P. Diblikova, J. Svoboda, A. Kovacik, K. Vavrova, J. Zbytovska, Int. J. Pharm. 2017, 534, 287; c) T. Uchino, I. Hatta, Y. Miyazaki, T. Onai, T. Yamazaki, F. Sugiura, Y. Kagawa, Int. J. Pharm. 2017, 521, 222; d) J. D. Bos, M. M. H. M. Meinardi, Exp. Dermatol. 2000, 9, 165.
- [10] P. R. Bergstresser, J. Richard Taylor, Br. J. Dermatol. 1977, 96, 503.
- [11] J. A. Bouwstra, M. Ponec, Biochim. Biophys. Acta, Biomembr. 2006, 1758, 2080.
- [12] A. S. Rzhevskiy, T. R. R. Singh, R. F. Donnelly, Y. G. Anissimov, J. Controlled Release 2018, 270, 184.
- [13] P. Karande, A. Jain, K. Ergun, V. Kispersky, S. Mitragotri, *Proc. Natl. Acad. Sci. U. S. A.* 2005, 102, 4688.
- [14] L. Margetts, R. Sawyer, BJA Educ. 2007, 7, 171.
- [15] G. M. El Maghraby, B. W. Barry, A. C. Williams, Eur. J. Pharm. Biopharm. 2008, 34, 203.
- [16] P.-W. Lee, S.-H. Hsu, J.-S. Tsai, F.-R. Chen, P.-J. Huang, C.-J. Ke, Z.-X. Liao, C.-W. Hsiao, H.-J. Lin, H.-W. Sung, Biomaterials 2010, 31, 2425
- [17] C. Yiyun, M. Na, X. Tongwen, F. Rongqiang, W. Xueyuan, W. Xiaomin, W. Longping, J. Pharm. Sci. 2007, 96, 595.
- [18] A. Marin, H. Sun, G. A. Husseini, W. G. Pitt, D. A. Christensen, N. Y. Rapoport, J. Controlled Release 2002, 84, 39.
- [19] Y. Talbi, E. Campo, D. Brulin, J. Y. Fourniols, *Electron. Lett.* 2018, 54, 739.
- [20] B. C. Q. Seah, B. M. Teo, Int. J. Nanomed. 2018, 13, 7749.
- [21] B. Zorec, S. Becker, M. Rebersek, D. Miklavcic, N. Pavselj, Int. J. Pharm. 2013, 457, 214.
- [22] a) J. W. Park, J. H. Park, Y. K. Yoon, Y. H. Joung, S. O. Choi, M. R. Prausnitz, M. G. Allen, in *Transducers '05*, *Digest of Technical Papers*, Vol. 2, IEEE, Piscataway, NJ 2005, pp. 1238–1241; b) J. W. Lee, P. Gadiraju, J. H. Park, M. G. Allen, M. R. Prausnitz, *J. Controlled Release* 2011, 154, 58.
- [23] D. L. Bremseth, F. Pass, Diabetes Technol. Ther. 2001, 3, 225.
- [24] M. J. Garland, K. Migalska, T. Mazlelaa, T. Mahmood, T. Raghu, R. Singh, A. D. Woolfson, R. F. Donnelly, Expert Rev. Med. Devices 2011, 8, 459.

- [25] A. C. Anselmo, Y. Gokarn, S. Mitragotri, Nat. Rev. Drug Discovery 2018, 18, 19.
- [26] X. Jin, D. D. Zhu, B. Z. Chen, M. Ashfaq, X. D. Guo, Adv. Drug Delivery Rev. 2018, 127, 119.
- [27] S. H. Bariya, M. C. Gohel, T. A. Mehta, O. P. Sharma, J. Pharm. Pharmacol. 2012, 64, 11.
- [28] S. Henry, D. V. McAllister, M. G. Allen, M. R. Prausnitz, J. Pharm. Sci. 1998, 87, 922.
- [29] a) W. Martanto, J. S. Moore, O. Kashlan, R. Kamath, P. M. Wang, J. M. O'Neal, M. R. Prausnitz, *Pharm. Res.* 2006, 23, 104; b) J. Gupta, E. I. Felner, M. R. Prausnitz, *Diabetes Technol. Ther.* 2009, 11, 329.
- [30] A. P. Raphael, M. L. Crichton, R. J. Falconer, S. Meliga, X. F. Chen, G. J. P. Fernando, H. Huang, M. A. F. Kendall, J. Controlled Release 2016, 225, 40.
- [31] J.-H. Park, M. G. Allen, M. R. Prausnitz, Pharm. Res. 2006, 23, 1008.
- [32] J.-H. Park, M. G. Allen, M. R. Prausnitz, J. Controlled Release 2005, 104, 51.
- [33] a) Q. Zhu, V. G. Zarnitsyn, L. Ye, Z. Wen, Y. Gao, L. Pan, I. Skountzou, H. S. Gill, M. R. Prausnitz, C. Yang, R. W. Compans, *Proc. Natl. Acad. Sci. U. S. A.* 2009, 106, 7968; b) P. C. DeMuth, J. J. Moon, H. Suh, P. T. Hammond, D. J. Irvine, ACS Nano 2012, 6, 8041.
- [34] K. Matsuo, S. Hirobe, Y. Yokota, Y. Ayabe, M. Seto, Y. S. Quan, F. Kamiyama, T. Tougan, T. Horii, Y. Mukai, N. Okada, S. Nakagawa, J. Controlled Release 2012, 160, 495.
- [35] S. P. Sullivan, N. Murthy, M. R. Prausnitz, Adv. Mater. 2008, 20, 933.
- [36] J. W. Lee, S.-O. Choi, E. I. Felner, M. R. Prausnitz, Small 2011, 7, 531.
- [37] M.-C. Chen, M.-H. Ling, K.-Y. Lai, E. Pramudityo, *Biomacromolecules* 2012, 13, 4022.
- [38] G. Li, A. Badkar, S. Nema, C. S. Kolli, A. K. Banga, *Int. J. Pharm.* 2009, 368, 109.
- [39] a) S. Yang, F. Wu, J. Liu, G. Fan, W. Welsh, H. Zhu, T. Jin, Adv. Funct. Mater. 2015, 25, 4633; b) Y. Zhang, G. Jiang, W. Yu, D. Liu, B. Xu, Mater. Sci. Eng., C 2018, 85, 18.
- [40] H.-W. Yang, L. Ye, X. D. Guo, C. Yang, R. W. Compans, M. R. Prausnitz, Adv. Healthcare Mater. 2017, 6, 1600750.
- [41] W. Chen, R. Tian, C. Xu, B. C. Yung, G. Wang, Y. Liu, Q. Ni, F. Zhang, Z. Zhou, J. Wang, G. Niu, Y. Ma, L. Fu, X. Chen, *Nat. Commun.* 2017, 8, 1777.
- [42] W. Yu, G. Jiang, Y. Zhang, D. Liu, B. Xu, J. Zhou, J. Mater. Chem. B 2017, 5, 9507.
- [43] H. Lee, T. K. Choi, Y. B. Lee, H. R. Cho, R. Ghaffari, L. Wang, H. J. Choi, T. D. Chung, N. S. Lu, T. Hyeon, S. H. Choi, D. H. Kim, *Nat. Nanotechnol.* 2016, 11, 566.
- [44] J. Yu, Y. Zhang, Y. Ye, R. DiSanto, W. Sun, D. Ranson, F. S. Ligler, J. B. Buse, Z. Gu, Proc. Natl. Acad. Sci. U. S. A. 2015, 112, 8260.
- [45] Y. Zhang, P. Feng, J. Yu, J. Yang, J. Zhao, J. Wang, Q. Shen, Z. Gu, Adv. Ther. 2018, 1, 1800035.
- [46] K. van der Maaden, W. Jiskoot, J. Bouwstra, J. Controlled Release 2012, 161, 645.
- [47] a) W. W. Lim, P. Wu, H. S. Bond, J. Y. Wong, K. W. Ni, W. H. Seto, M. Jit, B. J. Cowling, J. Global Antimicrob. Resist. 2019, 16, 17; b) H. Mulugeta, G. Dessie, F. Wagnew, D. Jara, C. T. Leshargie, A. Negesse, BMC Infect. Dis. 2019, 19, 383; c) A. Christensen, O. Kesti, V. Elenius, A. L. Eskola, H. Dollner, C. Altunbulakli, C. A. Akdis, M. Soderlund-Venermo, T. Jartti, Lancet Child Adolesc. Health 2019, 3, 418.
- [48] a) R. L. Creighton, K. A. Woodrow, Adv. Healthcare Mater. 2019, 8, 1801180; b) C. S. Hou, B. Yi, J. K. Jiang, Y. F. Chang, X. Yao, Biomater. Sci. 2019, 7, 822.
- [49] a) L. Yan, Y. Yang, W. J. Zhang, X. F. Chen, Adv. Mater. 2014, 26, 5533;
  b) S. Indermun, R. Luttge, Y. E. Choonara, P. Kumar, L. C. du Toit,
  G. Modi, V. Pillay, J. Controlled Release 2014, 185, 130.
- [50] a) X. N. Wang, N. McGovern, M. Gunawan, C. Richardson, M. Windebank, T. W. Siah, H. Y. Lim, K. Fink, J. L. Y. Li, L. G. Ng, F. Ginhoux, V. Angeli, M. Collin, M. Haniffa, J. Invest. Dermatol. 2014,

- 134, 965; b) G. M. Glenn, D. N. Taylor, X. R. Li, S. Frankel, A. Montemarano, C. R. Alving, *Nat. Med.* **2000**, *6*, 1403.
- [51] J. A. Mikszta, J. B. Alarcon, J. M. Brittingham, D. E. Sutter, R. J. Pettis, N. G. Harvey, *Nat. Med.* 2002, *8*, 415.
- [52] a) X. Chen, G. J. P. Fernando, M. L. Crichton, C. Flaim, S. R. Yukiko, E. J. Fairmaid, H. J. Corbett, C. A. Primiero, A. B. Ansaldo, I. H. Frazer, L. E. Brown, M. A. F. Kendall, J. Controlled Release 2011, 152, 349; b) C. Kolluru, Y. Gomaa, M. R. Prausnitz, Drug Delivery Transl. Res. 2019, 9, 192; c) M. J. Mistilis, A. S. Bommarius, M. R. Prausnitz, J. Pharm. Sci. 2015, 104, 740.
- [53] D. Poirier, F. Renaud, V. Dewar, L. Strodiot, F. Wauters, J. Janimak, T. Shimada, T. Nomura, K. Kabata, K. Kuruma, T. Kusano, M. Sakai, H. Nagasaki, T. Oyamada, *Biomaterials* 2017, 145, 256.
- [54] S. M. Bal, Z. Ding, E. van Riet, W. Jiskoot, J. A. Bouwstra, J. Controlled Release 2010, 148, 266.
- [55] a) X. F. Chen, H. J. Corbett, S. R. Yukiko, A. P. Raphael, E. J. Fairmaid, T. W. Prow, L. E. Brown, G. J. P. Fernando, M. A. F. Kendall, Adv. Funct. Mater. 2011, 21, 464; b) X. F. Chen, T. W. Prow, M. L. Crichton, D. W. K. Jenkins, M. S. Roberts, I. H. Frazer, G. J. P. Fernando, M. A. F. Kendall, J. Controlled Release 2009, 139, 212; c) H. J. Choi, D. G. Yoo, B. J. Bondy, F. S. Quan, R. W. Compans, S. M. Kang, M. R. Prausnitz, Biomaterials 2012, 33, 3756.
- [56] R. Haj-Ahmad, H. Khan, M. S. Arshad, M. Rasekh, A. Hussain, S. Walsh, X. Li, M. W. Chang, Z. Ahmad, *Pharmaceutics* 2015, 7, 486.
- [57] J. W. Lee, J. H. Park, M. R. Prausnitz, Biomaterials 2008, 29, 2113.
- [58] a) L. Yan, A. P. Raphael, X. Y. Zhu, B. L. Wang, W. Chen, T. Tang, Y. Deng, H. J. Sant, G. Y. Zhu, K. W. Choy, B. K. Gale, T. W. Prow, X. F. Chen, Adv. Healthcare Mater. 2014, 3, 555; b) A. P. Raphael, T. W. Prow, M. L. Crichton, X. F. Chen, G. I. P. Fernando, M. A. F. Kendall, Small 2010, 6, 1785.
- [59] a) W. Chen, C. Wang, L. Yan, L. B. Huang, X. Y. Zhu, B. Chen, H. J. Sant, X. R. Niu, G. Y. Zhu, K. N. Yu, V. A. L. Roy, B. K. Gale, X. F. Chen, J. Mater. Chem. B 2014, 2, 1699; b) S. P. Sullivan, D. G. Koutsonanos, M. D. Martin, J. W. Lee, V. Zarnitsyn, S. O. Choi, N. Murthy, R. W. Compans, I. Skountzou, M. R. Prausnitz, Nat. Med. 2010, 16, 915.
- [60] a) P. C. DeMuth, Y. Min, D. J. Irvine, P. T. Hammond, Adv. Health-care Mater. 2014, 3, 47; b) W. K. Raja, S. MacCorkle, I. M. Diwan, A. Abdurrob, J. Lu, F. G. Omenetto, D. L. Kaplan, Small 2013, 9, 3704.
- [61] R. C. Kines, V. Zarnitsyn, T. R. Johnson, Y. Y. S. Pang, K. S. Corbett, J. D. Nicewonger, A. Gangopadhyay, M. Chen, J. Liu, M. R. Prausnitz, J. T. Schiller, B. S. Graham, *PLoS One* **2015**, *10*, 0120797.
- [62] T. W. Prow, X. F. Chen, N. A. Prow, G. J. P. Fernando, C. S. E. Tan, A. P. Raphael, D. Chang, M. P. Ruutu, D. W. K. Jenkins, A. Pyke, M. L. Crichton, K. Raphaelli, L. Y. H. Goh, I. H. Frazer, M. S. Roberts, J. Gardner, A. A. Khromykh, A. Suhrbier, R. A. Hall, M. A. F. Kendall, Small 2010. 6, 1776.
- [63] S. Moon, Y. H. Wang, C. Edens, J. R. Gentsch, M. R. Prausnitz, B. M. Jiang, *Vaccine* 2013, 31, 3396.
- [64] a) H. S. Gill, J. Soderholm, M. R. Prausnitz, M. Sallberg, Gene Ther. 2010, 17, 811; b) M. B. P. Cuevas, M. Kodani, Y. Choi, J. Joyce, S. M. O'Connor, S. Kamili, M. R. Prausnitz, Bioeng. Transl. Med. 2018, 3, 186.
- [65] Y. Hiraishi, S. Nandakumar, S. O. Choi, J. W. Lee, Y. C. Kim, J. E. Posey, S. B. Sable, M. R. Prausnitz, *Vaccine* 2011, 29, 2626.
- [66] a) I.-J. Choi, A. Kang, M.-H. Ahn, H. Jun, S.-K. Baek, J.-H. Park, W. Na, S.-O. Choi, J. Controlled Release 2018, 286, 460; b) E. Q. Littauer, L. K. Mills, N. Brock, E. S. Esser, A. Romanyuk, J. A. Pulit-Penaloza, E. V. Vassilieva, J. T. Beaver, O. Antao, F. Krammer, R. W. Compans, M. R. Prausnitz, I. Skountzou, J. Controlled Release 2018, 276, 1.
- [67] C. Edens, M. L. Collins, J. Ayers, P. A. Rota, M. R. Prausnitz, *Vaccine* 2013, 31, 3403.
- [68] C. Edens, N. C. Dybdahl-Sissoko, W. C. Weldon, M. S. Oberste, M. R. Prausnitz, *Vaccine* 2015, 33, 4683.

- [69] M.-C. Chen, K.-Y. Lai, M.-H. Ling, C.-W. Lin, Acta Biomater. 2018, 65, 66.
- [70] P. C. DeMuth, A. V. Li, P. Abbink, J. Y. Liu, H. L. Li, K. A. Stanley, K. M. Smith, C. L. Lavine, M. S. Seaman, J. A. Kramer, A. D. Miller, W. Abraham, H. Suh, J. Elkhader, P. T. Hammond, D. H. Barouch, D. J. Irvine, Nat. Biotechnol. 2013, 31, 1082.
- [71] K. Ogurtsova, J. D. da Rocha Fernandes, Y. Huang, U. Linnenkamp, L. Guariguata, N. H. Cho, D. Cavan, J. E. Shaw, L. E. Makaroff, *Diabetes Res. Clin. Pract.* 2017, 128, 40.
- [72] a) M. A. Atkinson, G. S. Eisenbarth, A. W. Michels, *Lancet* 2014, 383, 69; b) M. Stumvoll, B. J. Goldstein, T. W. van Haeften, *Lancet* 2005, 365, 1333.
- [73] E. M. Cahill, S. Keaveney, V. Stuettgen, P. Eberts, P. Ramos-Luna, N. Zhang, M. Dangol, E. D. O'Cearbhaill, Acta Biomater. 2018, 80, 401.
- [74] W. Martanto, S. P. Davis, N. R. Holiday, J. Wang, H. S. Gill, M. R. Prausnitz, *Pharm. Res.* 2004, 21, 947.
- [75] S. P. Davis, W. Martanto, M. G. Allen, M. R. Prausnitz, *IEEE Trans. Biomed. Eng.* 2005, 52, 909.
- [76] D. Resnik, M. Možek, B. Pečar, A. Janež, V. Urbančič, C. Iliescu, D. Vrtačnik, Micromachines 2018, 9, 40.
- [77] E. Kochba, Y. Levin, I. Raz, A. Cahn, Diabetes Technol. Ther. 2016, 18, 525
- [78] S. Liu, J. Controlled Release 2012, 161, 933.
- [79] I. C. Lee, Y.-C. Wu, S.-W. Tsai, C.-H. Chen, M.-H. Wu, RSC Adv. 2017, 7. 5067.
- [80] B. Z. Chen, M. Ashfaq, D. D. Zhu, X. P. Zhang, X. D. Guo, Macromol. Rapid Commun. 2018, 39, 1800075.
- [81] M.-H. Ling, M.-C. Chen, Acta Biomater. 2013, 9, 8952.
- [82] M.-C. Chen, M.-H. Ling, S. J. Kusuma, Acta Biomater. 2015, 24, 106.
- [83] J. W. Lee, J.-H. Park, M. R. Prausnitz, Biomaterials 2008, 29, 2113.
- [84] S. Wang, M. Zhu, L. Zhao, D. Kuang, S. C. Kundu, S. Lu, ACS Biomater. Sci. Eng. 2019, 5, 1887.
- [85] a) D. Liu, B. Yu, G. Jiang, W. Yu, Y. Zhang, B. Xu, Mater. Sci. Eng., C 2018, 90, 180; b) W. Yu, G. Jiang, D. Liu, L. Li, Z. Tong, J. Yao, X. Kong, Mater. Sci. Eng., C 2017, 73, 425; c) W. Yu, G. Jiang, D. Liu, L. Li, H. Chen, Y. Liu, Q. Huang, Z. Tong, J. Yao, X. Kong, Mater. Sci. Eng., C 2017, 71, 725.
- [86] a) D. Liu, Y. Zhang, G. Jiang, W. Yu, B. Xu, J. Zhu, ACS Biomater. Sci. Eng. 2018, 4, 1687; b) Y. Zhang, G. Jiang, W. Hong, M. Gao, B. Xu, J. Zhu, G. Song, T. Liu, ACS Appl. Bio Mater. 2018, 1, 1906.
- [87] a) M. C. Chen, H. A. Chan, M. H. Ling, L. C. Su, J. Mater. Chem. B 2017, 5, 496; b) B. Xu, Q. Cao, Y. Zhang, W. Yu, J. Zhu, D. Liu, G. Jiang, ACS Biomater. Sci. Eng. 2018, 4, 2473; c) X. Hu, J. Yu, C. Qian, Y. Lu, A. R. Kahkoska, Z. Xie, X. Jing, J. B. Buse, Z. Gu, ACS Nano 2017, 11, 613; d) Z. Tong, J. Zhou, J. Zhong, Q. Tang, Z. Lei, H. Luo, P. Ma, X. Liu, ACS Appl. Mater. Interfaces 2018, 10, 20014; e) B. Xu, G. Jiang, W. Yu, D. Liu, Y. Zhang, J. Zhou, S. Sun, Y. Liu, J. Mater. Chem. B 2017, 5, 8200; f) J. Wang, Y. Ye, J. Yu, A. R. Kahkoska, X. Zhang, C. Wang, W. Sun, R. D. Corder, Z. Chen, S. A. Khan, J. B. Buse, Z. Gu, ACS Nano 2018, 12, 2466; g) S. Y. Chen, H. Matsumoto, Y. Moro-oka, M. Tanaka, Y. Miyahara, T. Suganami, A. Matsumoto, Adv. Funct. Mater. 2019, 29, 1807369.
- [88] Y. Zhang, J. Wang, J. Yu, D. Wen, A. R. Kahkoska, Y. Lu, X. Zhang, J. B. Buse, Z. Gu, Small 2018, 14, 1704181.
- [89] J. D. Kim, M. Kim, H. Yang, K. Lee, H. Jung, J. Controlled Release 2013, 170, 430.
- [90] H. Yang, S. Kim, I. Huh, S. Kim, S. F. Lahiji, M. Kim, H. Jung, Biomaterials 2015, 64, 70.
- [91] a) C. E. DeSantis, K. D. Miller, A. G. Sauer, A. Jemal, R. L. Siegel, Ca-Cancer J. Clin. 2019, 69, 211; b) R. L. Siegel, K. D. Miller, A. Jemal, Ca-Cancer J. Clin. 2019, 69, 7; c) F. Bray, J. Ferlay, I. Soerjomataram, R. L. Siegel, L. A. Torre, A. Jemal, Ca-Cancer J. Clin. 2018, 68, 394.
- [92] a) S. J. Zhao, G. L. Niu, F. Wu, L. Yan, H. Y. Zhang, J. F. Zhao, L. T. Zeng, M. H. Lan, J. Mater. Chem. B 2017, 5, 3651; b) J. C. Ge, Q. Y.

- Jia, W. M. Liu, M. H. Lan, B. J. Zhou, L. Guo, H. Y. Zhou, H. Y. Zhang, Y. Wang, Y. Gu, X. M. Meng, P. F. Wang, Adv. Healthcare Mater. 2016, 5, 665; c) J. F. Zhang, W. D. Nie, R. Chen, J. Chelora, Y. P. Wan, X. Cui, X. H. Zhang, W. J. Zhang, X. F. Chen, H. Y. Xie, C. S. Lee, Nano Lett. 2019, 19, 658; d) J. F. Zhang, C. X. Yang, R. Zhang, R. Chen, Z. Y. Zhang, W. J. Zhang, S. H. Peng, X. Y. Chen, G. Liu, C. S. Hsu, C. S. Lee, Adv. Funct. Mater. 2017, 27, 1605094; e) S. D. Shen, D. W. Jiang, L. Cheng, Y. Chao, K. Q. Nie, Z. L. Dong, C. J. Kutyreff, J. W. Engle, P. Huang, W. B. Cai, Z. Liu, ACS Nano 2017, 11, 9103; f) M. Lan, S. Zhao, W. Liu, C. S. Lee, W. Zhang, P. Wang, Adv. Healthcare Mater. 2019, 8, 1900132.
- [93] a) N. Muhamad, T. Plengsuriyakarn, K. Na-Bangchang, Int. J. Nanomed. 2018, 13, 3921; b) X. Liu, C. Liu, Z. Z. Zheng, S. Y. Chen, X. Pang, X. C. Xiang, J. X. Tang, E. Ren, Y. Z. Chen, M. You, X. Y. Wang, X. Y. Chen, W. X. Luo, G. Liu, N. S. Xia, Adv. Mater. 2019, 31, 1808294; c) H. Q. Song, F. F. Quan, Z. Q. Yu, M. H. Zheng, Y. Ma, H. H. Xiao, F. Ding, J. Mater. Chem. B 2019, 7, 433; d) Y. L. Wu, W. Y. Gu, Z. P. Xu, Nanomedicine 2019, 14, 77.
- [94] A. Lomas, J. Leonardi-Bee, F. Bath-Hextall, Br. J. Dermatol. 2012, 166, 1069.
- [95] a) M. C. F. Simoes, J. J. S. Sousa, A. Pais, Cancer Lett. 2015, 357, 8; b) H. W. Rogers, M. A. Weinstock, A. R. Harris, M. R. Hinckley, S. R. Feldman, A. B. Fleischer, B. M. Coldiron, Arch. Dermatol. 2010, 146, 283.
- [96] M. B. Lens, M. Dawes, Br. J. Dermatol 2004, 150, 179.
- [97] S. J. Welsh, P. G. Corrie, Ther. Adv. Med. Oncol. 2015, 7, 122.
- [98] M. C. Chen, Z. W. Lin, M. H. Ling, ACS Nano 2016, 10, 93.
- [99] H. P. Tham, K. Xu, W. Q. Lim, H. Chen, M. Zheng, T. G. S. Thng, S. S. Venkatraman, C. Xu, Y. Zhao, ACS Nano 2018, 12, 11936.
- [100] a) A. K. Jain, C. H. Lee, H. S. Gill, J. Controlled Release 2016, 239, 72;
  b) Y. Hao, M. Dong, T. Zhang, J. Peng, Y. Jia, Y. Cao, Z. Qian, ACS Appl. Mater. Interfaces 2017, 9, 15317;
  c) T. Jiang, T. Wang, T. Li, Y. Ma, S. Shen, B. He, R. Mo, ACS Nano 2018, 12, 9693;
  d) Q. Liu, M. Das, Y. Liu, L. Huang, Adv. Drug Delivery Rev. 2018, 127, 208;
  e) H. X. Nguyen, A. K. Banga, Pharm. Res. 2018, 35, 68;
  f) J. Pan, W. Ruan, M. Qin, Y. Long, T. Wan, K. Yu, Y. Zhai, C. Wu, Y. Xu, Sci. Rep. 2018, 8, 1117;
  g) W. Ruan, Y. Zhai, K. Yu, C. Wu, Y. Xu, Int. J. Pharm. 2018, 553, 298;
  h) K. S. Ahmed, X. Shan, J. Mao, L. Qiu, J. Chen, Mater. Sci. Eng., C 2019, 99, 1448;
  i) S. Bhatnagar, N. G. Bankar, M. V. Kulkarni, V. V. K. Venuganti, Int. J. Pharm. 2019, 556, 263.
- [101] L. Dong, Y. Li, Z. Li, N. Xu, P. Liu, H. Du, Y. Zhang, Y. Huang, J. Zhu, G. Ren, J. Xie, K. Wang, Y. Zhou, C. Shen, J. Zhu, J. Tao, ACS Appl. Mater. Interfaces 2018, 10, 9247.
- [102] X. Lan, J. She, ACS Appl. Mater. Interfaces 2018, 10, 33060.
- [103] X. Zhao, X. Li, P. Zhang, J. Du, Y. Wang, J. Controlled Release 2018, 286, 201.
- [104] a) C. Wang, Y. Q. Ye, Q. Y. Hu, A. Bellotti, Z. Gu, Adv. Mater. 2017, 29, 1606036; b) Y. Z. Min, K. C. Roche, S. M. Tian, M. J. Eblan, K. P. McKinnon, J. M. Caster, S. J. Chai, L. E. Herring, L. Z. Zhang, T. Zhang, J. M. DeSimone, J. E. Tepper, B. G. Vincent, J. S. Serody, A. Z. Wang, Nat. Nanotechnol. 2017, 12, 877; c) D. J. Irvine, M. A. Swartz, G. L. Szeto, Nat. Mater. 2013, 12, 978.
- [105] a) Q. Zeng, J. M. Gammon, L. H. Tostanoski, Y.-C. Chiu, C. M. Jewell, ACS Biomater. Sci. Eng. 2017, 3, 195; b) N. W. Kim, S.-Y. Kim, J. E. Lee, Y. Yin, J. H. Lee, S. Y. Lim, E. S. Kim, H. T. T. Duong, H. K. Kim, S. Kim, J.-E. Kim, D. S. Lee, J. Kim, M. S. Lee, Y. T. Lim, J. H. Jeong, ACS Nano 2018, 12, 9702.
- [106] R. J. Sullivan, K. T. Flaherty, Nat. Rev. Clin. Oncol. 2015, 12, 625.
- [107] C. Wang, Y. Ye, G. M. Hochu, H. Sadeghifar, Z. Gu, Nano Lett. 2016, 16, 2334.
- [108] Y. Ye, J. Wang, Q. Hu, G. M. Hochu, H. Xin, C. Wang, Z. Gu, ACS Nano 2016, 10, 8956.
- [109] D. Fernandes, Oral Maxillofac. Surg. Clin. North Am. 2005, 17, 51.

- [110] G. Fabbrocini, N. Fardella, A. Monfrecola, I. Proietti, D. Innocenzi, Clin. Exp. Dermatol. 2009, 34, 874.
- [111] K. Y. Park, H. K. Kim, S. E. Kim, B. J. Kim, M. N. Kim, Dermatol. Surg. 2012, 38, 1823.
- [112] S. Kim, M. Dangol, G. Kang, S. F. Lahiji, H. Yang, M. Jang, Y. Ma, C. Li, S. G. Lee, C. H. Kim, Y. W. Choi, S. J. Kim, J. H. Ryu, J. H. Baek, J. Koh, H. Jung, Mol. Pharmaceutics 2017, 14, 2024.
- [113] M. Kim, H. Yang, H. Kim, H. Jung, H. Jung, Int. J. Cosmet. Sci. 2014, 36, 207.
- [114] a) S. A. Coulman, J. C. Birchall, A. Alex, M. Pearton, B. Hofer, C. O'Mahony, W. Drexler, B. Považay, *Pharm. Res.* 2011, 28, 66; b) M. M. Badran, J. Kuntsche, A. Fahr, *Eur. J. Pharm. Biopharm.* 2009, 36, 511.
- [115] a) S. Doddaballapur, J. Cutaneous Aesthetic Surg. 2009, 2, 110; b) J. Sharad, J. Cosmet. Dermatol. 2011, 10, 317.
- [116] M. T. C. McCrudden, E. McAlister, A. J. Courtenay, P. González-Vázquez, T. R. Raj Singh, R. F. Donnelly, Exp. Dermatol. 2015, 24, 561.
- [117] Y. Hiraishi, T. Nakagawa, Y.-S. Quan, F. Kamiyama, S. Hirobe, N. Okada, S. Nakagawa, Int. J. Pharm. 2013, 441, 570.
- [118] S. Hirobe, H. Azukizawa, T. Hanafusa, K. Matsuo, Y.-S. Quan, F. Kamiyama, I. Katayama, N. Okada, S. Nakagawa, *Biomaterials* 2015, 57, 50.
- [119] W. Li, R. N. Terry, J. Tang, M. H. R. Feng, S. P. Schwendeman, M. R. Prausnitz, *Nat. Biomed. Eng.* 2019, 3, 220.
- [120] A. Than, C. H. Liu, H. Chang, P. K. Duong, C. M. G. Cheung, C. J. Xu, X. M. Wang, P. Chen, *Nat. Commun.* 2018, 9, 4433.
- [121] Y. Zhang, J. Yu, J. Wang, N. J. Hanne, Z. Cui, C. Qian, C. Wang, H. Xin, J. H. Cole, C. M. Gallippi, Y. Zhu, Z. Gu, Adv. Mater. 2017, 29, 1604043
- [122] a) L. E. G. Garcia, M. N. MacGregor, R. M. Visalakshan, N. Ninan, A. A. Cavallaro, A. D. Trinidad, Y. P. Zhao, A. J. D. Hayball, K. Vasilev, Chem. Commun. 2019, 55, 171; b) J. Xu, R. Danehy, H. Cai, Z. Ao, M. Pu, A. Nusawardhana, D. Rowe-Magnus, F. Guo, ACS Appl. Mater. Interfaces 2019, 11, 14640; c) P. Zan, A. Than, P.K. Duong, J. Song, C. Xu, P. Chen, Adv. Therap. 2019, https://doi.org/10.1002/adtp.201900064.
- [123] S. F. Lahiji, S. H. Seo, S. Kim, M. Dangol, J. Shim, C. G. Li, Y. Ma, C. Lee, G. Kang, H. Yang, K. Y. Choi, H. Jung, *Biomaterials* 2018, 167, 69.
- [124] X. Xie, C. Pascual, C. Lieu, S. Oh, J. Wang, B. D. Zou, J. L. Xie, Z. H. Li, J. Xie, D. C. Yeomans, M. X. Wu, X. S. Xie, ACS Nano 2017, 11, 395.
- [125] C. Tas, J. C. Joyce, H. X. Nguyen, P. Eangoor, J. S. Knaack, A. K. Banga, M. R. Prausnitz, J. Controlled Release 2017, 268, 159.
- [126] Y. Q. Zhang, Q. M. Liu, J. C. Yu, S. J. Yu, J. Q. Wang, L. Qiang, Z. Gu, ACS Nano 2017, 11, 9223.
- [127] a) P. Carter, B. Narasimhan, Q. Wang, Int. J. Pharm. 2019, 555, 49;
  b) K. S. Chaudhari, K. G. Akamanchi, ACS Biomater. Sci. Eng. 2018, 4, 4008;
  c) P. Dong, F. F. Sahle, S. B. Lohan, S. Saeidpour, S. Albrecht, C. Teutloff, R. Bodmeier, M. Unbehauen, C. Wolff, R. Haag, J. Lademann, A. Patzel, M. Schafer-Korting, M. C. Meinke, J. Controlled Release 2019, 295, 214;
  d) R. Gupta, B. Rai, Nanoscale 2018, 10, 4940;
  e) D. Park, J. Y. Lee, H. K. Cho, W. J. Hong, J. Kim, H. Seo, I. Choi, Y. Lee, J. Kim, S. J. Min, S. H. Yoon, J. S. Hwang, K. J. Cho, J. W. Kim, Biomacromolecules 2018, 19, 2682.
- [128] a) R. Chen, J. F. Zhang, J. Chelora, Y. Xiong, S. V. Kershaw, K. F. Li, P. K. Lo, K. W. Cheah, A. L. Rogach, J. A. Zapien, C. S. Lee, ACS Appl. Mater. Interfaces 2017, 9, 5699; b) J. C. Ge, M. H. Lan, B. J. Zhou, W. M. Liu, L. Guo, H. Wang, Q. Y. Jia, G. L. Niu, X. Huang, H. Y. Zhou, X. M. Meng, P. F. Wang, C. S. Lee, W. J. Zhang, X. D. Han, Nat. Commun. 2014, 5, 4596; c) J. F. Zhang, J. Zhang, W. Y. Li, R. Chen, Z. Y. Zhang, W. J. Zhang, Y. B. Tang, X. Y. Chen, G. Liu, C. S. Lee, Theranostics 2017, 7, 3007; d) L. Yan, X. F. Chen, Z. G. Wane,

www.advancedsciencenews.com

- X. J. Zhang, X. Y. Zhu, M. J. Zhou, W. Chen, L. B. Huang, V. A. L. Roy, P. K. N. Yu, G. Y. Zhu, W. J. Zhang, ACS Appl. Mater. Interfaces 2017, 9, 32990; e) A. Cifuentes-Rius, A. Ivask, E. Sporleder, I. Kaur, Y. Assan, S. Rao, D. Warther, C. A. Prestidge, J. O. Durand, N. H. Voelcker, Small 2017, 13, 1701201; f) D. X. Zhang, C. Yoshikawa, N. G. Welch, P. Pasic, H. Thissen, N. H. Voelcker, Sci. Rep. 2019, 9, 1367
- [129] a) D. Maiti, X. M. Tong, X. Z. Mou, K. Yang, Front. Pharmacol. 2019, 9, 1401; b) K. Olszowska, J. B. Pang, P. S. Wrobel, L. Zhao, H. Q. Ta, Z. F. Liu, B. Trzebicka, A. Bachmatiuk, M. H. Rummeli, Synth. Met. 2017, 234, 53; c) K. Yang, L. Z. Feng, H. Hong, W. B. Cai, Z. Liu, Nat. Protoc. 2013, 8, 2392; d) F. J. Harding, S. Surdo, B. Delalat, C. Cozzi, R. Elnathan, S. Gronthos, N. H. Voelcker, G. Barillaro, ACS Appl. Mater. Interfaces 2016, 8, 29197; e) T. Tieu, M. Alba, R. Elnathan, A. Cifuentes-Rius, N. H. Voelcker, Adv. Ther. 2019, 2, 1800095; f) M. Alba, B. Delalat, P. Formentín, M.-L. Rogers, L. F. Marsal, N. H. Voelcker, Small 2015, 11, 4626.
- [130] a) Y. X. Wang, L. H. Feng, S. Wang, Adv. Funct. Mater. 2019, 29, 133;
  b) N. Lu, L. Q. Wang, M. Lv, Z. S. Tang, C. H. Fan, Nano Res. 2019, 12, 247;
  c) L. Yan, J. F. Zhang, C. S. Lee, X. F. Chen, Small 2014, 10, 4487;
  d) G. B. Qi, Y. J. Gao, L. Wang, H. Wang, Adv. Mater. 2018, 30, 1703444;
  e) X. Q. Chen, J. Sun, H. Zhao, K. Yang, Y. D. Zhu, H. R. Luo, K. Yu, H. S. Fan, X. D. Zhang, J. Mater. Chem. B 2018, 6, 3586;
  f) X. Q. Chen, Y. J. Tang, A. M. Liu, Y. D. Zhu, D. Gao, Y. Yang, J. Sun, H. S. Fan, X. D. Zhang, ACS Appl. Mater. Interfaces 2018, 10, 14378.
- [131] a) A. E. Nel, L. Madler, D. Velegol, T. Xia, E. M. V. Hoek, P. Somasundaran, F. Klaessig, V. Castranova, M. Thompson, *Nat. Mater.* 2009, 8, 543; b) R. Elnathan, B. Delalat, D. Brodoceanu, H. Alhmoud, F. J. Harding, K. Buehler, A. Nelson, L. Isa, T. Kraus, N. H. Voelcker, *Adv. Funct. Mater.* 2015, 25, 7215.
- [132] R. Jijie, A. Barras, R. Boukherroub, S. Szunerits, J. Mater. Chem. B 2017, 5, 8653.
- [133] R. Goyal, L. K. Macri, H. M. Kaplan, J. Kohn, J. Controlled Release 2016, 240, 77.
- [134] J. M. Caster, A. N. Patel, T. Zhang, A. Wang, Wiley Interdiscip. Rev.: Nanomed. Nanobiotechnol. 2017, 9, e1416.
- [135] a) V. R. Leite-Silva, M. L. Lamer, W. Y. Sanchez, D. C. Liu, W. H. Sanchez, I. Morrow, D. Martin, H. D. T. Silva, T. W. Prow, J. E. Grice, M. S. Roberts, Eur. J. Pharm. Biopharm. 2013, 84, 297; b) S. Nafisi, M. Schäfer-Korting, H. I. Maibach, Nanotoxicology 2015, 9, 643.
- [136] a) J. Liu, R. Zhang, Z.P. Xu, Small 2019, 15, e1900262; b) X. Li, A.M. Aldayel, Z. Cui, J. Controlled Release 2014 173, 148. c) W. Chen, H. Zuo, B. Rolfe, M.A. Schembri, R.N. Cobbold, B. Zhang, T.J. Mahony, Z.P. Xu, J. Controlled Release 2018, 292, 196. d) M. Massaro, G. Cavallaro, C. G. Colletti, G. D'Azzo, S. Guernelli, G. Lazzara, S. Pieraccini, S. Riela, J. Colloid Interface Sci. 2018, 524, 156; e) L. Yang, J. Lv, Y. Li, J. Yang, B. Zhang, S. Li, J. Yang, ACS Appl. Bio Mater. 2018, 1, 328
- [137] a) A. Jose, S. Labala, K. M. Ninave, S. K. Gade, V. V. K. Venuganti, AAPS PharmSciTech 2018, 19, 166; b) A. Jose, S. Labala, V. V. K. Venuganti, J. Drug Targeting 2017, 25, 330; c) O. S. Muddineti, P. Kumari, B. Ghosh, V. P. Torchilin, S. Biswas, ACS Appl. Mater. Interfaces 2017, 0, 16778
- [138] Y. F. Rao, W. Chen, X. G. Liang, Y. Z. Huang, J. Miao, L. Liu, Y. Lou, X. G. Zhang, B. Wang, R. K. Tang, Z. Chen, X. Y. Lu, Small 2015, 11, 239
- [139] C. Wiraja, Y. Zhu, D. C. S. Lio, D. C. Yeo, M. Xie, W. N. Fang, Q. Li, M. J. Zheng, M. Van Steensel, L. H. Wang, C. H. Fan, C. J. Xu, Nat. Commun. 2019, 10, 12.
- [140] a) J. F. Lin, J. Li, A. Gopal, T. Munshi, Y. W. Chu, J. X. Wang, T. T. Liu, B. Y. Shi, X. F. Chen, L. Yan, *Chem. Commun.* 2019, 55, 2656; b) Y. W. Xi, J. Ge, Y. Guo, B. Lei, P. X. Ma, *ACS Nano* 2018, 12, 10772.

- [141] a) R. Schiavelli, M. Ajzenszlos, D. Di Tullio, N. R. Campoverde, E. Maiolo, F. Margulis, N. Gomez, R. Sabbatiello, M. Pattin, M. Rano, Rev. Nefrol. Dial. Tras. 2019, 39, 15; b) M. Heckel, S. Stiel, F. A. Herbst, J. M. Tiedtke, A. Sturm, T. Adelhardt, C. Bogdan, C. Sieber, O. Schoffski, F. R. Lang, C. Ostgathe, Supportive Care Cancer 2018, 26, 3021; c) C. C. Herrera, E. Cordova, L. Morganti, W. Cornistein, F. Garibaldi, N. Gomez, M. Badia, C. Rodriguez, Int. J. Infect. Dis. 2018, 73, 15.
- [142] a) B. Le Ouay, F. Stellacci, Nano Today 2015, 10, 339; b) R. T. Zhao, M. Lv, Y. Li, M. X. Sun, W. Kong, L. H. Wang, S. P. Song, C. H. Fan, L. L. Jia, S. F. Qiu, Y. S. Sun, H. B. Song, R. Z. Hao, ACS Appl. Mater. Interfaces 2017, 9, 15328; c) S. H. Tang, J. Zheng, Adv. Healthcare Mater. 2018, 7, 1701503.
- [143] a) R. B. Vasani, E. J. Szili, G. Rajeev, N. H. Voelcker, *Chem. Asian J.*2017, 12, 1605; b) H. Alhmoud, B. Delalat, X. Ceto, R. Elnathan, A. Cavallaro, K. Vasilev, N. H. Voelcker, *RSC Adv.* 2016, 6, 65976; c) E. J. Kwon, M. Skalak, A. Bertucci, G. Braun, F. Ricci, E. Ruoslahti, M. J. Sailor, S. N. Bhatia, *Adv. Mater.* 2017, 29, 1701527.
- [144] H. Alhmoud, A. Cifuentes-Rius, B. Delalat, D. G. Lancaster, N. H. Voelcker, ACS Appl. Mater. Interfaces 2017, 9, 33707.
- [145] a) D. Mao, F. Hu, Kenry, S. Ji, W. Wu, D. Ding, D. Kong, B. Liu, Adv. Mater. 2018, 30, e1706831; b) Z. Y. Song, Y. Wu, Q. Cao, H. J. Wang, X. R. Wang, H. Y. Han, Adv. Funct. Mater. 2018, 28, 1800011;
  c) B. H. Neufeld, M. J. Neufeld, A. Lutzke, S. M. Schweickart, M. M. Reynolds, Adv. Funct. Mater. 2017, 27, 1702255; d) M. Liu, L. Wang, X. H. Zheng, Z. G. Xie, ACS Appl. Mater. Interfaces 2017, 9, 41512.
- [146] a) C. M. Courtney, S. M. Goodman, J. A. McDaniel, N. E. Madinger, A. Chatterjee, P. Nagpal, *Nat. Mater.* 2016, 15, 529; b) W. Y. Yin, J. Yu, F. T. Lv, L. Yan, L. R. Zheng, Z. J. Gu, Y. L. Zhao, *ACS Nano* 2016, 10, 11000; c) X. Fan, F. Yang, C. X. Nie, Y. Yang, H. F. Ji, C. He, C. Cheng, C. S. Zhao, *ACS Appl. Mater. Interfaces* 2018, 10, 296.
- [147] Y. Li, X. M. Liu, L. Tan, Z. D. Cui, X. J. Yang, Y. F. Zheng, K. W. K. Yeung, P. K. Chu, S. L. Wu, Adv. Funct. Mater. 2018, 28, 1800299.
- [148] a) Y. Zhao, Q. Q. Guo, X. M. Dai, X. S. Wei, Y. J. Yu, X. L. Chen, C. X. Li, Z. Q. Cao, X. E. Zhang, Adv. Mater. 2019, 31, 1806024; b) Y. Li, Y. Tian, W. S. Zheng, Y. Feng, R. Huang, J. X. Shao, R. B. Tang, P. Wang, Y. X. Jia, J. J. Zhang, W. F. Zheng, G. Yang, X. Y. Jiang, Small 2017, 13, 1700130; c) X. L. Yang, J. C. Yang, L. Wang, B. Ran, Y. X. Jia, L. M. Zhang, G. Yang, H. W. Shao, X. Y. Jiang, ACS Nano 2017, 11, 5737.
- [149] a) F. F. Xiao, B. Cao, C. Y. Wang, X. J. Guo, M. G. Li, D. Xing, X. L. Hu, ACS Nano 2019, 13, 1511; b) X. Pang, Q. C. Xiao, Y. Cheng, E. Ren, L. L. Lian, Y. Zhang, H. Y. Gao, X. Y. Wang, W. N. Leung, X. Y. Chen, G. Liu, C. S. Xu, ACS Nano 2019, 13, 2427.
- [150] H. Han, J. Zhu, D. Q. Wu, F. X. Li, X. L. Wang, J. Y. Yu, X. H. Qin, Adv. Funct. Mater. 2019, 29, 1806594.
- [151] J. L. Huang, J. F. Zhou, J. Y. Zhuang, H. Z. Gao, D. H. Huang, L. X. Wang, W. L. Wu, Q. B. Li, D. P. Yang, M. Y. Han, ACS Appl. Mater. Interfaces 2017, 9, 36606.
- [152] J. X. Wang, H. J. Zhou, G. Y. Guo, J. Q. Tan, Q. J. Wang, J. Tang, W. Liu, H. Shen, J. H. Li, X. L. Zhang, ACS Appl. Mater. Interfaces 2017, 9, 33609.
- [153] C. T. Turner, M. Hasanzadeh Kafshgari, E. Melville, B. Delalat, F. Harding, E. Mäkilä, J. J. Salonen, A. J. Cowin, N. H. Voelcker, ACS Biomater. Sci. Eng. 2016, 2, 2339.
- [154] Z. Zhang, Y. Liu, Y. S. Chen, L. X. Li, P. Lan, D. N. He, J. Song, Y. X. Zhang, ACS Appl. Mater. Interfaces 2019, 11, 3704.
- [155] F. B. Rabello, C. D. Souza, J. A. Farina, Clinics 2014, 69, 565.
- [156] G. Yang, H. E. Lee, S. W. Shin, S. H. Um, J. D. Lee, K. B. Kim, H. C. Kang, Y. Y. Cho, H. S. Lee, J. Y. Lee, Adv. Funct. Mater. 2018, 28, 1801018
- [157] a) J. E. Koo, S. W. Shin, S. H. Um, J. Y. Lee, Mol. Cancer 2015, 14, 104; b) S. H. Um, J. B. Lee, N. Park, S. Y. Kwon, C. C. Umbach, D. Luo, Nat. Mater. 2006, 5, 797.



#### www.advancedsciencenews.com

**ADVANCED**THERAPEUTICS

- [158] D. Son, J. Lee, S. Qiao, R. Ghaffari, J. Kim, J. E. Lee, C. Song, S. J. Kim, D. J. Lee, S. W. Jun, S. Yang, M. Park, J. Shin, K. Do, M. Lee, K. Kang, C. S. Hwang, N. S. Lu, T. Hyeon, D. H. Kim, *Nat. Nanotechnol.* 2014, 9, 397.
- [159] P. Q. Cai, W. R. Leow, X. Y. Wang, Y. L. Wu, X. D. Chen, Adv. Mater. 2017, 29, 1605529.
- [160] A. K. Yetisen, J. L. Martinez-Hurtado, B. Unal, A. Khademhosseini, H. Butt, Adv. Mater. 2018, 30, 1706910.
- [161] K. Ita, Pharmaceutics 2015, 7, 90;

- [162] Y. Zhang, J. Yu, A. R. Kahkoska, J. Wang, J. B. Buse, Z. Gu, Adv. Drug Delivery Rev. 2018, 139, 51.
- [163] N. G. Rouphael, M. Paine, R. Mosley, S. Henry, D. V. McAllister, H. Kalluri, W. Pewin, P. M. Frew, T. Yu, N. J. Thornburg, S. Kabbani, L. Lai, E. V. Vassilieva, I. Skountzou, R. W. Compans, M. J. Mulligan, M. R. Prausnitz, T.-M. S. Group, *Lancet* 2017, 390, 649.
- [164] M. A. Botelho, D. B. Queiroz, G. Barros, S. Guerreiro, P. Fechine, S. Umbelino, A. Lyra, B. Borges, A. Freitas, D. C. Queiroz, R. Ruela, J. G. Almeida, L. Quintans, Jr., Clinics 2014, 69, 75.